

University of Nebraska - Lincoln

DigitalCommons@University of Nebraska - Lincoln

Dissertations & Theses in Natural Resources

Natural Resources, School of


5-2017

Integration of Hydrogeophysical Datasets for Improved Water Resource Management in Irrigated Systems

Catherine E. Finkenbiner

University of Nebraska-Lincoln, c.finkenbiner@gmail.com

Follow this and additional works at: <http://digitalcommons.unl.edu/natresdiss>

 Part of the [Agriculture Commons](#), [Hydrology Commons](#), [Natural Resources and Conservation Commons](#), [Natural Resources Management and Policy Commons](#), [Other Environmental Sciences Commons](#), and the [Water Resource Management Commons](#)

Finkenbiner, Catherine E., "Integration of Hydrogeophysical Datasets for Improved Water Resource Management in Irrigated Systems" (2017). *Dissertations & Theses in Natural Resources*. 145.

<http://digitalcommons.unl.edu/natresdiss/145>

This Article is brought to you for free and open access by the Natural Resources, School of at DigitalCommons@University of Nebraska - Lincoln. It has been accepted for inclusion in Dissertations & Theses in Natural Resources by an authorized administrator of DigitalCommons@University of Nebraska - Lincoln.

Integration of Hydrogeophysical Datasets for Improved Water
Resource Management in Irrigated Systems

by

Catherine E. Finkenbiner

A THESIS

Presented to the Faculty of
The Graduate College at the University of Nebraska
In Partial Fulfillment of Requirements
For the Degree of Master of Science
Major: Natural Resource Sciences
Under the Supervision of Professor Trenton E. Franz
Lincoln, Nebraska

May 2017

Integration of Hydrogeophysical Datasets for Improved Water Resource Management in Irrigated Systems

Catherine E. Finkenbiner, M.S.

University of Nebraska, 2017

Advisor: Trenton Franz

Water scarcity is predicted to be the major limitation to increasing agronomic outputs to meet future food and fiber demands. With the agricultural sector accounting for 80 – 90% of all consumptive water use and an average water use efficiency (WUE) of less than 45%, major advances must be made in irrigation water management. Precision agriculture, specifically variable-rate irrigation (VRI) and variable-speed irrigation (VSI) systems, offers the technologies to address and manage for infield variability and incorporate that into management decisions. The major limitation to implementing this technology often lies in the management of spatial datasets and the development of irrigation prescription maps that address variables impacting yield and soil moisture. While certain datasets and mapping technologies exist in practice, this study explored the utility of the recently developed cosmic-ray neutron probe (CRNP) which measures soil water content (SWC) in the top ~30cm of the soil profile. The key advantages of CRNP are that the sensor is passive, non-invasive, mobile and soil temperature-invariant, making data collection more compatible with existing farm operations and extending the mapping period. The objectives of this study were to: 1) improve the delineation of

management zones within a field and 2) estimate spatial soil hydraulic properties (i.e. field capacity and wilting point) to make effective irrigation prescription maps. To accomplish this, a series of CRNP SWC surveys were collected in a 53-ha field near Sutherland, Nebraska. The SWC surveys were analyzed using Empirical Orthogonal Functions (EOF) to isolate the underlying spatial structure. Results indicated the measured SWC at field capacity and wilting point were better correlated to CRNP EOF as compared to other commonly used datasets. Based on this work, a soil sampling strategy and CRNP EOF analysis was proposed for better quantifying soil hydraulic properties. While the proposed strategy will increase overall effort as compared to traditional techniques, rising scrutiny for agricultural water-use may increase the adoption of this technology.

Acknowledgements

First, I would like to thank the University of Nebraska Extension for awarding me a Graduate Student Assistantship and their continual support throughout my graduate studies. The University of Nebraska Extension team provided me with invaluable educational and networking experiences including attendance to conferences, meeting with producers and industry, and collaboration with extension faculty and staff across the state.

This research would not have been successful without funding support from the Monsanto Graduate Student Scholarship. Not only did this scholarship help pay for my education, I was able to purchase a computer and laboratory equipment essential for the completion of this thesis. The scholarship also provided me with the opportunity to attend two conferences: the American Geophysical Union Fall Meeting 2015 in San Francisco, California and the 2016 European Geosciences Union in Vienna, Austria.

I would like to thank my advisor Dr. Trenton Franz for his knowledge and support the last four years as I completed my undergraduate and progressed into a Master's degree. His feedback throughout the completion of this thesis not only made me a better academic but also a better scientist. With his support, I was given the opportunity to participate in a wide variety of fieldwork and research projects. Dr. Franz helped me prepare poster and oral presentations for multiple research conferences in the United States and one in Europe. His assistance and guidance provided me with the skills to be successful in my future endeavors.

I would like to thank my committee members: Dr. Derek Heeren, Dr. Joe Luck, and Dr. Nathan Mueller. Their knowledge, experience and recommendations contributed to the success of my research and completion of this thesis. I am forever grateful to them for their time and commitment to this project.

Thank you to Justin Gibson for your wisdom and patience teaching me how to use the laboratory equipment fundamental for the completion of this thesis. A special thank you to Paulman Farms for access to field sites, crop datasets and logistical support. Thank you to Matthew Russell for helping me collect the soil samples used in this study.

Lastly, I would like to thank my family and friends for their support throughout my M.S. degree. I would especially like to thank my parents who have always encouraged and supported me throughout my academic career.

Table of Contents

Abstract	ii
Acknowledgements	iv
Table of Figures	vii
Table of Tables	ix
List of Abbreviations	x
Chapter 1: Foreword	1
Chapter 2: Integration of Hydrogeophysical Datasets for Improved Water Resource Management in Irrigated Systems	3
2.1 Introduction	3
2.2 Materials & Methods	8
2.2.1 Study Site	8
2.2.2 Hydrogeophysical Datasets	11
2.2.3 Soil Sampling and Laboratory Analysis	13
2.3 Results and Discussion	14
2.3.1 Hydrogeophysical Sampling and EOF Analysis	14
2.3.2 Soil Sampling and Laboratory Analysis	18
2.3.3 Comparison of Landscape Position and Hydrogeophysical Datasets with Laboratory Analysis	21
2.3.4 Recommendation for Future Soil Hydraulic Property Sampling	25
2.4 Conclusion	27
Chapter 3: Conclusions & Future Directions	29
References	32
Appendix	36

Table of Figures

Figure 2.1: Conceptual diagram of potential reductions in pumping versus effort for various soil hydraulic datasets/techniques.

Figure 2.2: Field site located near Sutherland, NE (field center: 41.065393°, -101.102663°), illustrating latitude, longitude, soil core sampling locations (black dots), 1m elevation contours and the calculated topographic wetness index (TWI).

Figure 2.3: The USDA SSURGO soil descriptions and their respective soil water content (SWC) at field capacity and wilting point.

Figure 2.4: Apparent electrical conductivity map (ECa) collected on 24 February 2016 using a Dualem-21S sensor.

Figure 2.5: Ten CRNP rover SWC surveys collected between March 2015 and June 2016.

Figure 2.6: The first EOF surface depicting the underlying dominant spatial structure created from the ten CRNP rover SWC surveys in Figure 2.5.

Figure 2.7: Soil water retention functions from three undisturbed soil cores. Values before pF (log of tension, (MPa)) of 3 were recorded using the Decagon Hyprop and values after a pF of 3 were recorded using a WP4C Dewpoint PotentialMeter.

Figure 2.8: Laboratory measured SWC at field capacity (FC) and wilting point (WP) compared to AWC, elevation, TWI, measured ECa, and the first EOF surface from the CRNP rover SWC surveys.

Figure 2.9: Resulting spatial estimates of SWC at a) field capacity and b) wilting point using derived relationship between laboratory measured soil hydraulic parameters and the first EOF surface.

Figure S2.1: Soil water retention functions for undisturbed soil core samples 1, 2, 3 and 4. Values before pF (log of tension, (MPa)) of 2.8 were recorded using the Decagon Hyprop and values after a pF of 2.8 were recorded using a WP4C Dewpoint PotentiaMeter.

Figure S2.2: Soil water retention functions for undisturbed soil core samples 5, 6, 7 and 8. Values before pF (log of tension, (MPa)) of 3 were recorded using the Decagon Hyprop and values after a pF of 3 were recorded using a WP4C Dewpoint PotentiaMeter.

Figure S2.3: Soil water retention functions for undisturbed soil core samples 9, 10, 11 and 12. Values before pF (log of tension, (MPa)) of 3 were recorded using the Decagon Hyprop and values after a pF of 3 were recorded using a WP4C Dewpoint PotentiaMeter.

Figure S2.4: Soil water retention functions for undisturbed soil core samples 13, 14, 15 and 16. Values before pF (log of tension, (MPa)) of 3 were recorded using the Decagon Hyprop and values after a pF of 3 were recorded using a WP4C Dewpoint PotentiaMeter.

Figure S2.5: Soil water retention functions for undisturbed soil core samples 17, 18, 19 and 20. Values before pF (log of tension, (MPa)) of 3 were recorded using the Decagon Hyprop and values after a pF of 3 were recorded using a WP4C Dewpoint PotentiaMeter.

Figure S2.6: Soil water retention functions for undisturbed soil core samples 21, 22, 23 and 24. Values before pF (log of tension, (MPa)) of 3 were recorded using the Decagon Hyprop and values after a pF of 3 were recorded using a WP4C Dewpoint PotentiaMeter.

Figure S2.7: Soil water retention functions for undisturbed soil core samples 25, 26, 27 and 28. Values before pF (log of tension, (MPa)) of 3 were recorded using the Decagon Hyprop and values after a pF of 3 were recorded using a WP4C Dewpoint PotentiaMeter.

Figure S2.8: Soil water retention functions for undisturbed soil core samples 29, 30, and 31. Values before pF (log of tension, (MPa)) of 3 were recorded using the Decagon Hyprop and values after a pF of 3 were recorded using a WP4C Dewpoint PotentiaMeter.

Figure S2.9: MatLab (.m) script used to generated soil retention function figures for the undisturbed soil cores.

Table of Tables

Table 2.1: Summary of undisturbed soil core locations and associated values.

Table 2.2: Linear regression r^2 and RMSE for measured SWC at field capacity, measured SWC at wilting point and calculated AWC versus elevation, TWI, ECa map and EOF surface.

List of Abbreviations

<u>Abbreviation</u>	<u>Description</u>
ATV	All-terrain Vehicle
AWC	Available Water Content
AWDN	Automated Weather Data Network
CRNP	Cosmic-ray Neutron Probe
EC	Electrical Conductivity
ECa	Apparent Electrical Conductivity
EOF	Empirical Orthogonal Function
FC	Field Capacity
IMZ	Irrigation Management Zone
MAD	Maximum Allowable Depletion
MUKEY	Mapping Unit Symbol
NRD	Natural Resource District
PTF	Pedotransfer Function
RMSE	Root Mean Square Error
SIS	Soil Information System
SSURGO	USDA Web Soil Survey Soil Spatial Dataset
SWC	Soil Water Content
TWI	Topographic Wetness Index
USDA	United States Department of Agriculture
VRI	Variable-rate Irrigation
VSI	Variable-speed Irrigation
WP	Wilting Point
WUE	Water-use Efficiency

Chapter 1: Foreword

According to a 2007 U.S. Department of Agriculture (USDA) Census of Agriculture report, Nebraska ranks first nationally in irrigated area with approximately 3.4 million irrigated hectares. Nebraska has about 100,000 registered irrigation wells and 16,000 registered water wells (USDA 2007). A majority of irrigators pump groundwater from the critical and depleting High Plains Aquifer to irrigate their crops. Natural Resource Districts (NRD) and policy makers allocate water polices in the state in an effort to manage groundwater depletion and recharge rates. Many NRDs in Nebraska enforce stringent pumping restrictions.

Center-pivot irrigation accounts for approximately 72% of the irrigated area in Nebraska (USDA 2007). Conventional center pivot systems manage a field as a uniform unit, thus ignoring the heterogeneity across the field. Therefore, management decisions are typically based on average field conditions (McCarthy et al. 2014). Consequently, regions of a field will vary in yield due to variations in soil moisture and physical properties. Technological advances in site-specific crop management have the potential to greatly improve water use efficiency (WUE). Precision agriculture, specifically variable-rate irrigation (VRI) and variable-speed irrigation (VSI) systems, can vary irrigation application depth in relation to the spatial variability of soil properties (Hezarjaribi and Sourell 2007). The major limitation in implementing this technology often lies in the management of spatial datasets and the development of irrigation prescription maps that address variables impacting yield and soil moisture (Evans et al. 1996). This requires efficient and accurate methods for measuring the spatial variability of soil properties including porosity, saturated hydraulic conductivity, unsaturated

hydraulic conductivity, texture and depth (Hezarjaribi and Sourell 2007; Ranney et al. 2015). Managing irrigation rates and times based on hydraulic properties allows for irrigators to prescribe application depths based on the soil water content (SWC) below field capacity and above maximum allowable depletion (MAD), or the maximum amount of plant available water allowed to be removed from the soil before precipitation or irrigation refill occurs. Furthermore, identifying in-field variability and irrigation management zones (IMZs) is vital for minimizing runoff and deep percolation, especially in drought years.

The goal of this research was to increase our understanding of soil hydrologic fluxes for field-scale management. The study objectives were to 1) improve the delineation of IMZs within a field and 2) estimate the relevant spatially-distributed soil hydraulic properties (i.e. field capacity and wilting point) to inform irrigation prescriptions. Traditional IMZ delineation techniques (i.e. soil spatial datasets, electrical conductivity (EC) maps) and the cosmic-ray neutron probe (CRNP) rover were used to characterize the spatial variability of soil properties for a popcorn field irrigated with a VRI pivot near Sutherland, NE. Laboratory measured soil hydraulic properties from thirty-one undisturbed soil cores were compared to the soil spatial datasets, EC map, and CRNP analysis. Chapter 2 of this thesis has been submitted for publication in the Precision Agriculture journal.

Chapter 2: Integration of Hydrogeophysical Datasets for Improved Water Resource Management in Irrigated Systems

2.1 Introduction

Water scarcity is predicted to be the major limitation to increasing agronomic outputs to meet future food and fiber demands (UNDP 2007). With the agricultural sector accounting for 80 – 90% of all consumptive water use and an average water use efficiency (WUE) of less than 45% (Hezarjaribi and Sourell 2007; Molden 2007), major advances must be made in irrigation water management. Currently, irrigation is a key component of global food security, accounting for ~40% of global food production and ~20% of all arable land (Molden 2007; Schultz et al. 2005). Precision agriculture offers the technologies to address and manage for infield variability and incorporate that variability into management decisions (Howell et al. 2012).

According to a 2007 U.S. Department of Agriculture (USDA) Census of Agriculture report, Nebraska ranks first nationally in irrigated area approximately 3.4 million irrigated hectares, and about 72% of that area has center pivot irrigation (USDA 2007). Conventional center pivot systems manage a field as a uniform unit, thus ignoring the heterogeneity across the field, and often management decisions are based on average field conditions (McCarthy et al. 2014). Consequently, expected crop yield may differ in sub-regions of a field due to variations in soil moisture and physical properties. Variable-rate irrigation (VRI) and variable-speed irrigation (VSI) systems can vary application depth in relation to the spatial variability of soil properties (Hezarjaribi and Sourell

2007). VSI varies the speed of the pivot to adjust application depth in sectors, and VRI uses nozzle control to vary application depth in irregularly shaped management zones. Additionally, fertigation inputs can also be managed for site-specific field conditions and soil properties to ensure minimal chemical loss in the runoff (Hedley 2015). Due to the high temporal variability in soil moisture, the incorporation of VRI has the potential to increase crop WUE and yield (Haghverdi et al. 2015b). The major limitation to implementing this technology often lies in the management of spatial datasets and the writing of irrigation prescription maps that address variables impacting yield and soil moisture (Evans et al. 1996; Howell et al. 2012). This requires efficient and accurate methods for measuring the field scale spatial variability of soil properties including porosity, saturated hydraulic conductivity, unsaturated hydraulic conductivity, available water, texture and depth (Hezarjaribi and Sourell 2007; Pan et al. 2013; Ranney et al. 2015). Managing irrigation rates and times based on hydraulic properties allows for irrigators to prescribe application depths based on the soil water content (SWC) below field capacity and above maximum allowable depletion.

Land managers use several methods to address and manage for in-field variability and to delineate irrigation management zones (IMZs) including available soil spatial datasets, electrical resistivity/conductivity (EC) surveys, and commercially available instruments. Unfortunately, soil spatial datasets are often not at resolutions appropriate for field-scale management (Bobryk et al. 2016). One strategy which land managers will use is delineating IMZs within a field based on EC surveys. High resolution spatiotemporal modeling using EC surveys has been used to characterize dynamic soil moisture patterns in relation to crop needs (Hedley et al. 2013). Unfortunately, EC is

sensitive to temperature, SWC, texture, clay content and salinity (Haghverdi et al. 2015a; Rodriguez-Perez et al. 2011). While changes in SWC do account for over 50% of variability in soil EC readings (Brevik et al. 2006), the dynamic nature of SWC causes EC and clay measurements to vary temporally (McCutcheon et al. 2006) making the use of a single EC survey problematic. One commercially available EC instrument, the Trimble Soil Information System (SIS) (Trimble Inc., Sunnyvale, CA), measures soil physical and chemical variability and is used within agricultural management to optimize the use of water, fertilizer and amendment application. SIS offers 3D soil models of root zone depth, soil texture, water holding capacity, compaction characteristics, nutrient levels, and salt and toxicity concentrations. However, these spatial products are subject to the field conditions at the time of EC sampling.

Beyond EC surveys, other hydrogeophysical instruments (Binley et al. 2015) offer promising opportunities in precision agriculture. One such instrument to be explored in this work is the cosmic-ray neutron probe (CRNP), which has been used within agricultural systems to approximate SWC at the field- to small-watershed-scale (Franz et al. 2015). For this study, the CRNP was used to measure SWC at high spatial and temporal resolutions to characterize its dynamic nature over the growing season. One key advantage to using the passive, non-invasive, and soil-temperature-invariant CRNP method is that SWC data can be collected using a wide variety of commercially available vehicles from harvest until the following season when the crop too tall for the vehicle (~0.20 m for this work). While not performed here, surveys with taller crop heights can easily be collected from taller-bodied farm equipment (i.e. tractor, sprayer, etc.). Most EC systems are used to delineate management zones only after harvest and before planting in

nonfrozen soils, thus limiting mapping opportunities in cold climates. Also in this work, a standard multivariate analysis, empirical orthogonal functions (EOF, (Perry and Niemann 2006)), was used to characterize the spatial variability of SWC across the study site using CRNP surveys collected between 2015-2016. EOF analyses have been proven to be an accurate method for large sample sizes or more than five days of SWC monitoring (Werbylo and Niemann 2014). Within intensely monitored agricultural systems, EOF analysis has also been used to identify dominant parameters controlling spatial and temporal patterns of surface SWC without being affected by a single random process (Korres et al. 2010). Furthermore, EOF analysis provides a framework to estimate underlying SWC variations constructed using historical SWC observations to forecast SWC patterns for unobserved times.

The objectives of this study were to: 1) improve the delineation of management zones within a field and 2) estimate the relevant spatially-distributed soil hydraulic properties (i.e. field capacity and wilting point) to inform irrigation prescriptions. Measured hydraulic parameters were compared to values from the USDA soil survey dataset, an EC map and the CRNP-derived EOF surface to investigate which dataset correlated best. The CRNP surveys, when combined with the EOF analysis, were hypothesized to be the best predictor of laboratory-measured soil hydraulic property spatial variability compared to traditional and widely-used methods. It was also hypothesized that the EOF surface would be a good candidate for more accurately delineating IMZs. To illustrate the potential reduction in pumping versus effort (i.e. time, energy, and cost) of the various strategies discussed, Figure 2.1 presents a conceptual diagram with a nonlinear curve and a set of existing technologies/methodologies. The

figure serves as a guide to the reader and will be further discussed later in this paper with respect to the specific findings from this field site.

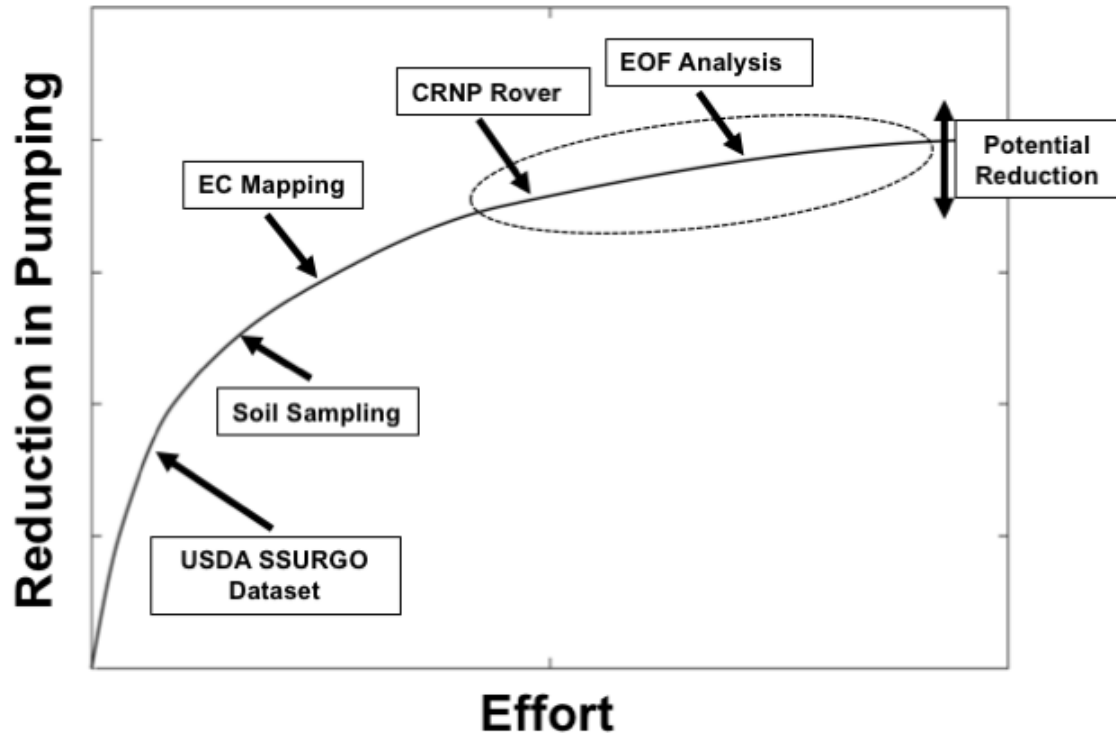


Figure 2.1: Conceptual diagram of potential reductions in pumping versus effort for various soil hydraulic datasets/techniques.

2.2 Materials and Methods

2.2.1 Study Site

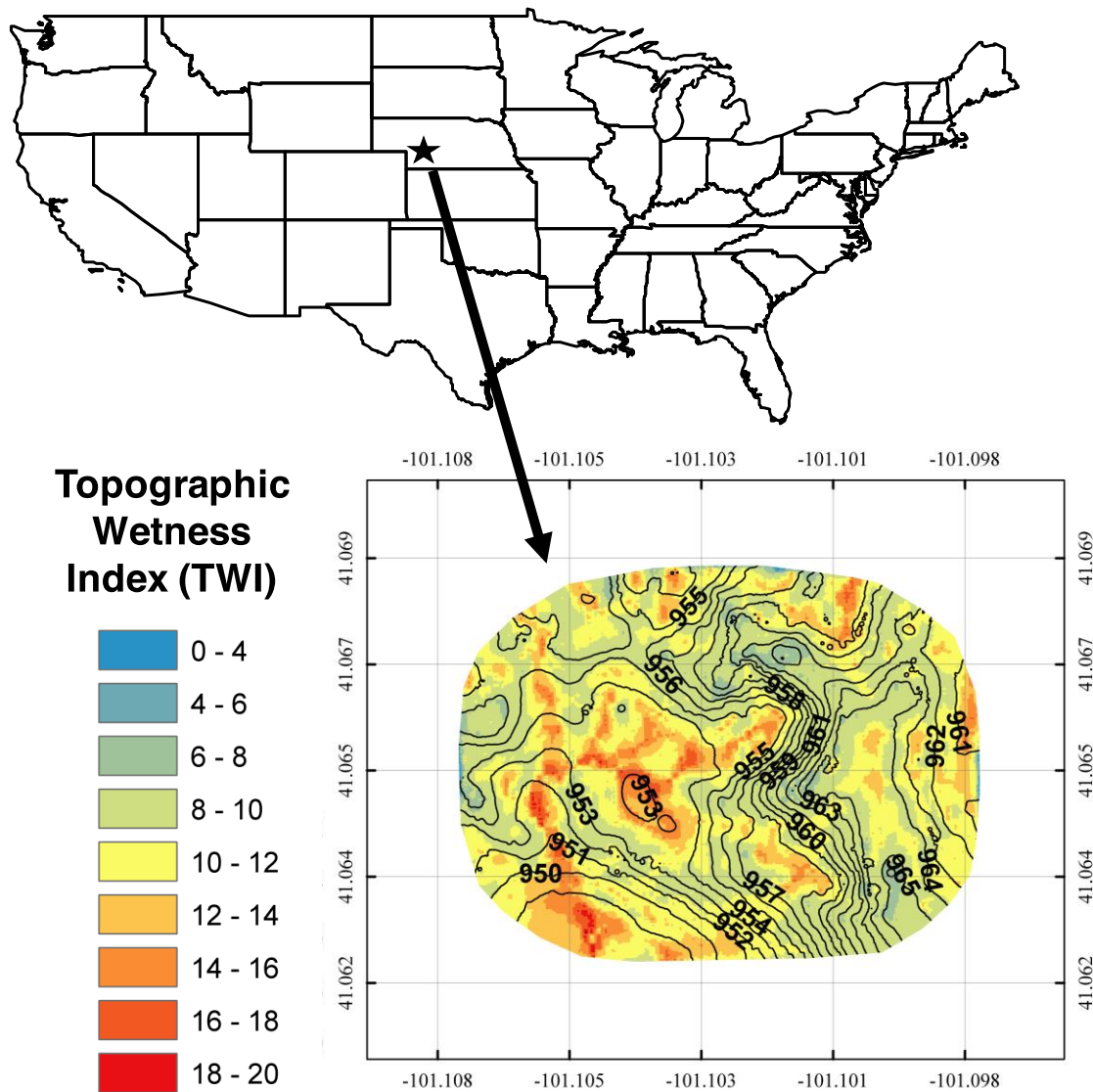
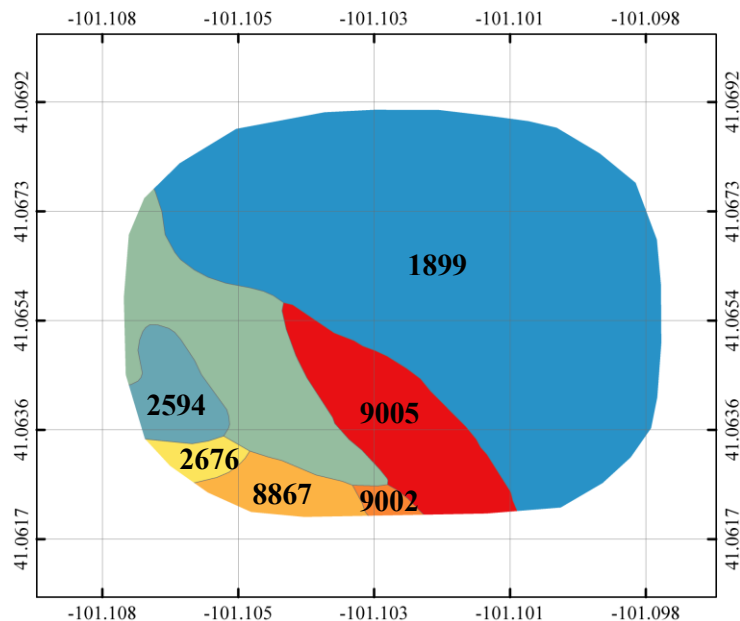


Figure 2.2: Field site located near Sutherland, NE (field center: 41.065393° , -101.102663°), illustrating latitude, longitude, soil core sampling locations (black dots), 1m elevation contours and the calculated topographic wetness index (TWI).

The selected study site is a 53-hectare field irrigated with a VRI pivot near Sutherland, NE (41.065393° , -101.102663°) (Fig. 2). The field contains significant topo-edaphic

gradients making it an ideal candidate for VRI. Fig. 2 also illustrates the elevation (provided by a local crop consultant using a RTK GPS) and topographic wetness index (TWI; Sorensen et. al. 2006) of the study site. The field was planted with soybean (*glycine max*) in 2014 and popcorn maize (*zea mays everta*) from 2015-2016. The soybean yield averaged ~4.3 t/ha and the popcorn yields averaged ~5.8 t/ha. Using data from an Automated Weather Data Network (AWDN) site located near North Platte, NE (~40 km from study site), the authors estimated annual temperature highs to be around 18°C and lows to be about 2°C (<http://www.hprcc.unl.edu/awdn.php>, Accessed 25 January 2017). The authors used the AWDN dataset to estimate decadal annual average precipitation at 445 mmyr⁻¹ with 325 mm falling between May and September. Additionally, the authors estimated potential annual evapotranspiration to be at 1475 mmyr⁻¹ with 925 mm occurring between May and September. According to the local producer, applied irrigation varies between 150 to 300 mmyr⁻¹ depending on the year. Soil classifications from the available USDA SSURGO (Soil Survey Staff, 2016) spatial and tabular dataset were used to estimate texture and soil hydraulic properties at the study site. SWC at field capacity (cm³cm⁻³), correlating to a soil water pressure of -33 kPa, and wilting point (cm³cm⁻³), correlating to a soil water pressure of -1500 kPa, were averaged for each of the map units from 0 - 0.3m (Fig. 3). The USDA SSURGO database delineated contiguous areas with similar soils as a single map unit. In general, the eastern region of the field has sandier soils and the western region is a mixture of sandy and silt loams. The field has a wide gradient in field capacity and wilting point values depending on soil classification. The TWI product (Fig. 2) correlates well with the classifications from the SSURGO dataset with wetter regions of the field relating to finer soil textures.



MUSYM	Soil Description	SWC (cm ³ cm ⁻³) at -33kPa	SWC (cm ³ cm ⁻³) at -1500kPa
1899	Valent sand, rolling	0.090	0.027
2594	Hersh and Valentine (fine sand) soils, 6-11% slopes	0.168	0.068
2601	Hersh soils (well drained sandy loam), 3-6% slopes	0.193	0.100
2676	Holdrege silt loam, 3-7% slopes, eroded, plains and breaks	0.307	0.164
8867	Hord fine sandy loam, 1-3% slopes	0.225	0.125
9002	Anselmo fine sandy loam, 1-3% slopes	0.204	0.112
9005	Anselmo fine sandy loam, 6-9% slopes	0.206	0.112

Figure 2.3: The USDA SSURGO soil descriptions and their respective SWC at field capacity and wilting point.

2.2.2 Hydrogeophysical datasets

An apparent EC (ECa) map was collected on 24 February 2016 using a DUALEM-21S sensor (DUALEM, Milton, Canada). The DUALEM sensor has dual-geometry receivers at separations of 1- and 2-m from the transmitter, which provided four simultaneous depth estimates of bulk ECa (mSm^{-1}) every second (DuaLEM Inc. 2013). The DUALEM was towed behind an all-terrain vehicle (ATV) on a plastic sled at speeds of $8\text{-}15 \text{ kmhr}^{-1}$ with $\sim 7 - 9 \text{ m}$ spacing, taking about 75 minutes to complete the survey. A Hemisphere GPS XF101 DGPS (Juniper Systems, Inc., Logan, UT) unit recorded the location of each measurement. Following basic quality assurance and quality control of the raw ECa data (Franz et al. 2011), a spatial map with 5 by 5 m resolution was created using an inverse-distance weighting procedure. Note that the 2 m horizontal co-planar signal was used for ECa in subsequent analyses.

Ten mobile CRNP surveys to estimate SWC were completed at the site from March 2015 - June 2016 using an ATV driven in a similar pattern and rate as the previously described EC survey. The mobile CRNP records epithermal neutron intensity integrated over one minute counting intervals. The change in epithermal neutron intensity is inversely correlated to the mass of hydrogen in the measurement volume (Zreda et al. 2012). SWC changes are by far the largest change in hydrogen mass (McJannet et al. 2014). Numerous validation studies across the globe (see Franz et al. 2011; Bogena et al. 2013; Hawdon et al. 2014; Franz et al. 2016) have shown the CRNP to have area-average measurement accuracies of less than $0.03 \text{ cm}^3\text{cm}^{-3}$ against a variety of industry standard SWC point scale probes. The measurement volume is roughly a disk, with a $\sim 250 \text{ m}$ radius circle and penetration depth of 0.15 to 0.40 m (Köhli et al. 2015) depending on

local conditions. For simplicity, a constant penetration depth of 0.3 m was assumed for all surveys. In order to provide a SWC map, first a spatial map of neutron intensity was estimated, then a calibration function was applied following details in Franz et al. (2015) for agricultural fields. The neutron intensity map is created in two steps. First, a drop-in-the-bucket preprocessing step is applied, where a dense grid is generated (here 20 by 20 m) and all raw data points are found within a certain radius (here 50 m). Then, the average of all raw data found within the search radius is assigned it to the grid center. This oversampling approach is necessary for sharpening the image quality and is a common strategy used in remote sensing analyses (see Chan et al. 2014) when overlapping area average observations are collected, like the CRNP in this study. Next, an inverse-distance-weighted approach is used on the resampled 20 m grid to provide the 5-m neutron intensity estimate. Finally, the neutron intensity gridded estimate is converted to SWC following Franz et al. (2015). The authors refer the reader to the rapidly growing CRNP literature (see Zreda et al. 2012) instead of providing full details of the methodology here.

In order to illuminate the underlying spatial variability of the SWC maps, an EOF analysis was used on the ten CRNP SWC maps. Full details on the multivariate statistical EOF analysis are provided elsewhere (Korres et al. 2010; Perry and Niemann 2006) and only a brief summary is provided here. The EOF analysis decomposes the observed SWC variability measured by the CRNP surveys into a set of orthogonal spatial patterns (EOFs), which are invariant in time, and a set of time series called expansion coefficients, which are invariant in space (Perry and Niemann 2006). Multiplication of the EOFs and expansion coefficients will exactly reconstruct the original pattern. Often the number of

needed coefficients (i.e. eigenvectors) to reconstruct most of the data is less than the original dataset (i.e. determined by the ranked eigenvalues), thus the procedure can be used as a way to reduce the dimensionality of the dataset while preserving the key information. The authors note that EOF is nearly identical to Principal Component Analysis, save the splitting of axis of variation into spatial and temporal coefficients instead of arbitrary linear combinations.

2.2.3 Soil sampling and laboratory analysis

Thirty-one sample locations (Figure 2.2) were chosen based on the SSURGO database soil classifications, EC map and EOF analysis in a stratified random sampling scheme. Undisturbed soil cores (250 cm³) were collected inside stainless steel cylinders at ~0.2 m depth at each sample location. The soil cores were placed in a cooler and transported back to the laboratory where they were stored in a 4°C refrigerator for storage until analyzed. Soil water retention curves were estimated for each of the soil cores using a Decagon HYPROP (Decagon Devices, Pullman, WA, USA). Saturated soil samples were exposed to evaporation in the laboratory and weighed throughout the experiment. Evaporation methods are proven to be a fast and reliable method for determining soil hydraulic properties within the saturated to moderate SWC range (Peters and Durner 2008; Schindler et al. 2010). The matric head was continuously monitored by two tensiometers inserted at the base of the soil cores at two different lengths within the core. The tensiometers and instrument bases were degassed using a vacuum pump. The HYPROP software (Decagon Devices, Pullman, WA, USA) calculated data points along the retention curve and unsaturated hydraulic conductivity curve. An average measured

bulk density of 1.62 gcm^{-3} and porosity of 38.9% were assigned for each of the undisturbed samples to generate soil water retention curves. Following the HYPROP analysis, a WP4C Dewpoint Potential Meter (Decagon Devices, Pullman, WA, USA) was used to approximate tension for the moderate to dry SWC ranges. The soil cores were dried at 105°C for 24 hours before collecting 1 - 9 sub-samples per sample. Varying volumes of water were added to the sub-samples to obtain SWC near wilting point and to further characterize the soil water retention curves. The sub-samples were sealed for 24 hours after water was added to allow for the water to disperse evenly throughout the sub-sample. Inside the measurement chamber of the WP4C, the dew point temperature of the moist air was measured by a chilled mirror and the sample temperature was measured by an infrared thermometer. Those two values were then used to calculate relative humidity and thus, potential of the soil water. The WP4C has an accuracy of $\pm 0.05 \text{ MPa}$ from 0 to -5 MPa and 1% from -5 to -300 MPa (Decagon Devices, Inc. 2015).

2.3 Results and Discussion

2.3.1 Hydrogeophysical mapping and EOF analysis

The ECa map for the field is illustrated in Figure 2.4 and provides additional spatial information on soil texture variability as compared to the USDA SSURGO map. This type of information has been used for the delineation of IMZs (Pan et al. 2013). As noted previously, the ECa map is subject to field conditions at the time of the sampling. Therefore, areas of high EC measurements in the southwest quadrant of the field may be due to increased soil cations, SWC, and/or temperature anomalies at the time of sampling. At a first look, the delineated soil boundaries by the USDA SSURGO database

display some spatial correlation to the ECa map. However, there is high variability of ECa values within each USDA SSURGO soil classification, which has been observed in other research (Brevik et al. 2006). Thus, the soil classification from the SSURGO dataset may or may not be the appropriate boundaries for IMZs within the field. This uncertainty of exact IMZ boundaries and questionable repeatability of ECa makes this method problematic, particularly given the high initial capital for precision agricultural equipment. The result here suggests the use of soil survey datasets and ECa be used in tandem to delineate IMZs for precision agriculture, which is supported by the results of Brevik et al. (2006).

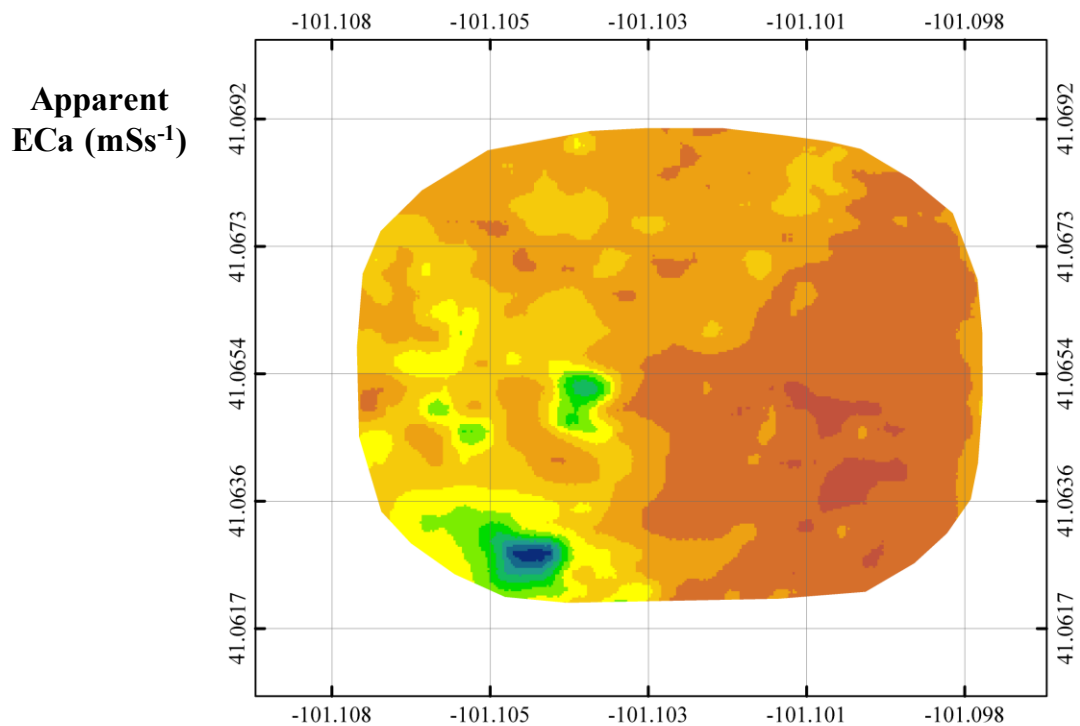


Figure 2.4: Apparent electrical conductivity map (ECa) collected on 24 February 2016 using a Dualem-21S sensor.

Figure 2.5 illustrates the large spatiotemporal variation in SWC over the ten dates observed using the CRNP rover. The regions of the field with finer soil textures and higher ECa generally have a higher SWC in each of the soil moisture maps. The ten CRNP rover surveys were used to perform EOF analysis. Here the first EOF coefficients explained 79.6% of the spatial SWC variability followed by 5.6% explained by the second EOF. Therefore, only the first EOF was considered in the subsequent analyses. Figure 2.6 illustrates the first EOF coefficients at the study site. Statistical bootstrapping of the SWC also indicated that five CRNP surveys at different SWC conditions were sufficient to estimate the first EOF coefficients to within 5% of the values using data from all ten surveys. This reduction in required number of CRNP surveys is critical for economic considerations beyond a research study. The first EOF map provides detailed information for the delineation of IMZs. Given the removal of the time-varying component of the signal the authors argue that the map is a superior method to delineate IMZs as compared to the USDA SSURGO dataset and ECa mapping. The first EOF map is a continuous surface; thus, it can be applied at a variety of spatial scales and used within existing agricultural management software (such as a shapefile input). The remaining questions whether it really is a better predictor of soil hydraulic properties and whether the improvement is economical for a producer to undertake in practice.

SWC ($\text{cm}^3\text{cm}^{-3}$)

0.0 - 0.05

0.05 - 0.10

0.10 - 0.15

0.15 - 0.20

0.20 - 0.25

0.25 - 0.30

0.30 - 0.35

0.35 - 0.40

0.40 - 0.45

0.45 - 0.50

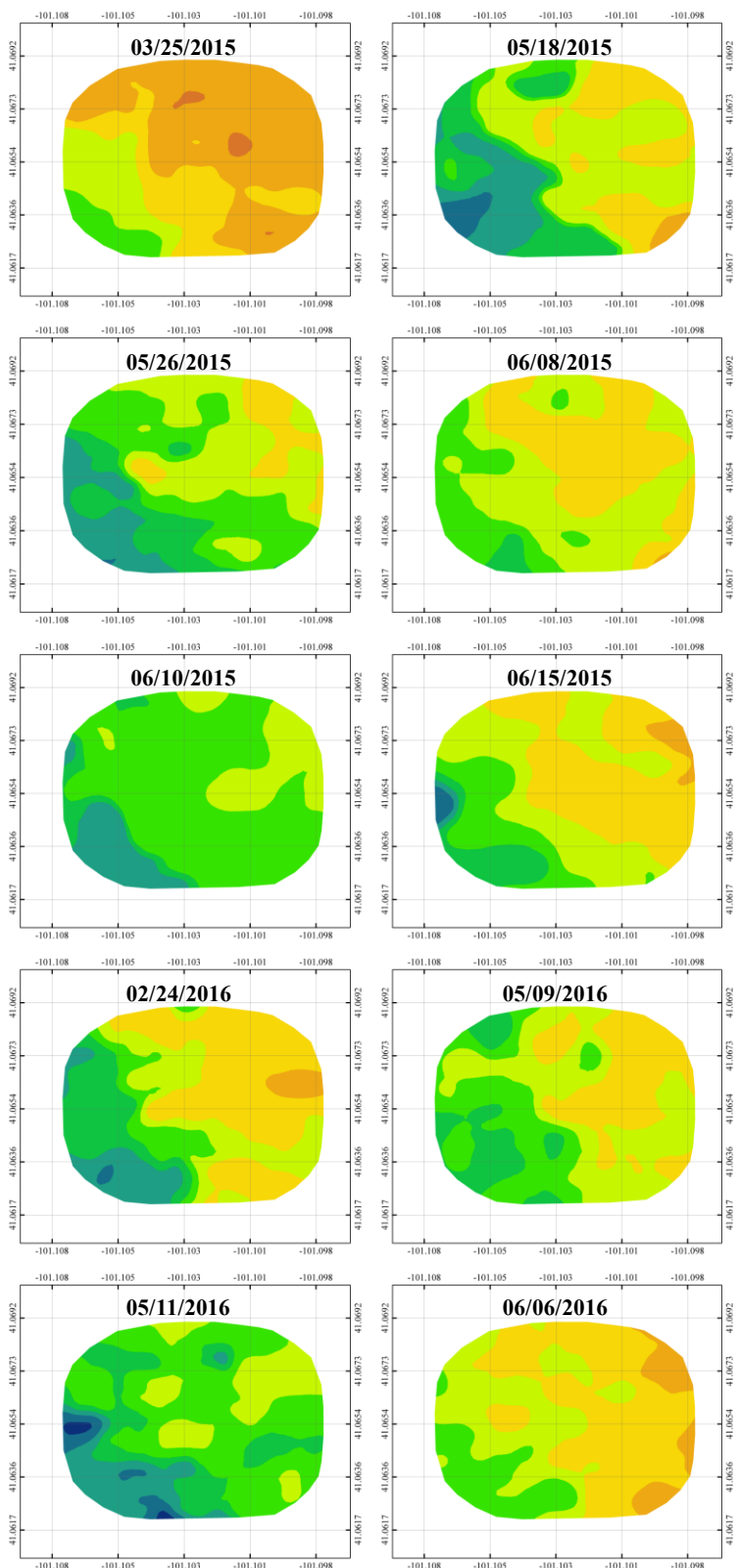


Figure 2.5: Ten CRNP rover SWC surveys collected between March 2015 and June 2016.

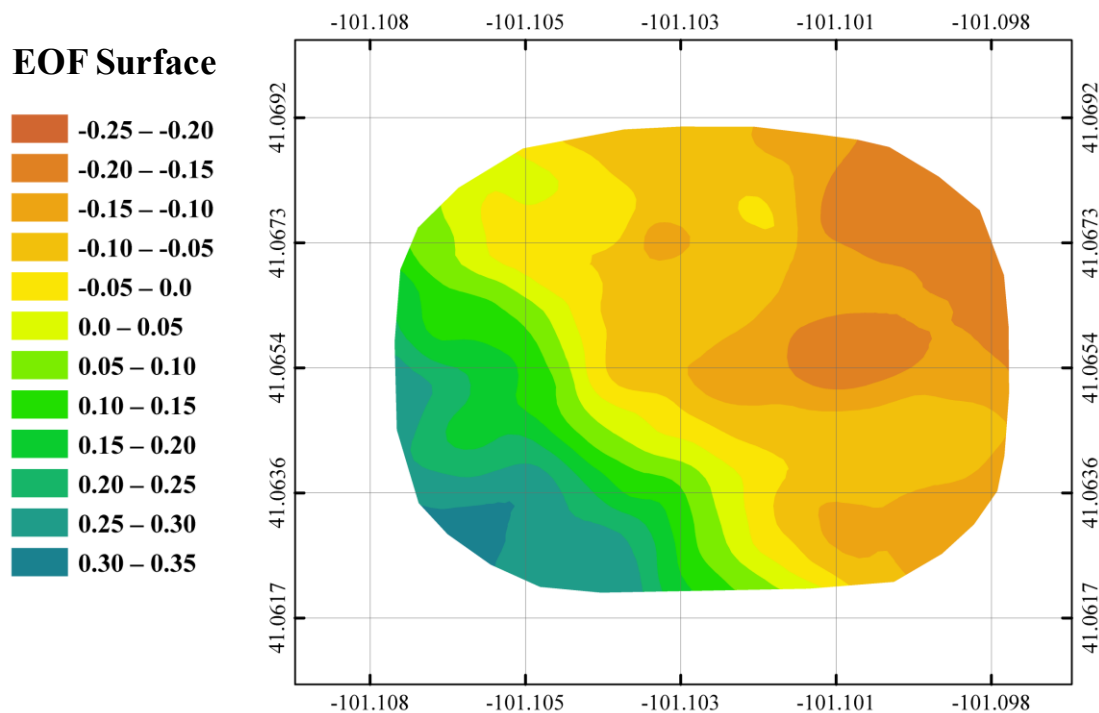


Figure 2.6: The first EOF surface depicting the underlying dominant spatial structure created from the ten CRNP rover SWC surveys in Figure 2.5.

2.3.2 Soil sampling and laboratory analysis

Using each of the thirty-one undisturbed soil cores, soil hydraulic properties were estimated from soil water retention curves generated using the Hyprop software. To illustrate the type of data generated, three of the soil cores and their respective field capacity and wilting point values are shown in Figure 2.7. Table 2.1 summarizes the SWC at field capacity (-33kPa), SWC at wilting point (-1500kPa) and calculated AWC for each of the thirty-one soil cores. In general, areas of the field with lower EOF values also have lower SWC at field capacity and wilting point. Additionally, SWC at field

capacity and wilting point is higher for finer soils and lower in coarser texture classes.

AWC is higher for areas of the field with finer textured soils.

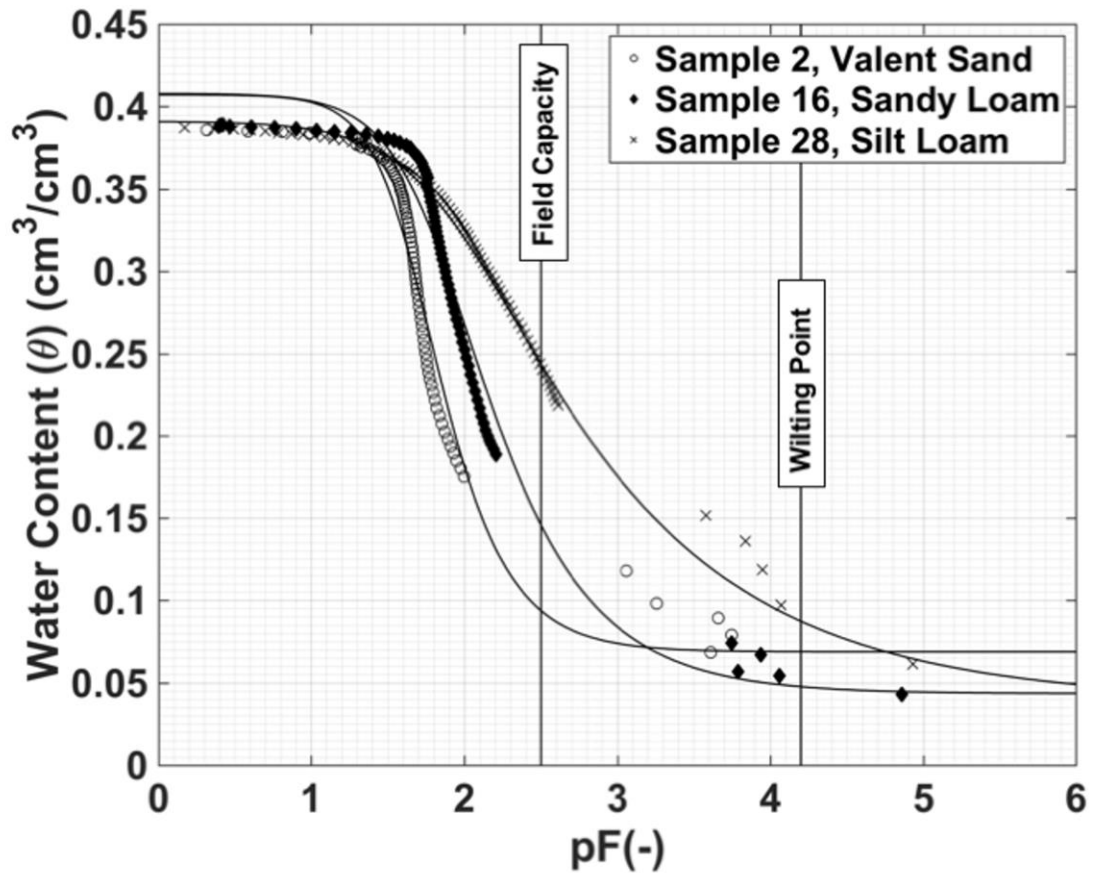


Figure 2.7: Soil water retention functions from three undisturbed soil cores. Values before pF (log of tension, (MPa)) of 3 were recorded using the Decagon Hyprop and values after a pF of 3 were recorded using a WP4C Dewpoint PotentiaMeter.

Sample Number	Latitude (°)	Longitude (°)	Elevation (m)	TWI	SSURGO Database			Apparent ECa (mSm ⁻¹)	CRNP Rover EOF	Measured SWC (cm ³ cm ⁻³) at			AWC (cm ³ cm ⁻³)
					MUKEY	SWC (cm ³ cm ⁻³) at 33 kPa	SWC (cm ³ cm ⁻³) at 1500 kPa			6 kPa	33 kPa	1500 kPa	
1	41.068212	-101.100420	958.74	12.73	1899	0.090	0.027	41.20	-0.1787	0.286	0.096	0.080	0.016
2	41.067437	-101.099080	961.77	10.49	1899	0.090	0.027	33.36	-0.1992	0.259	0.092	0.069	0.023
3	41.066830	-101.100055	962.92	10.09	1899	0.090	0.027	31.73	-0.1382	0.305	0.112	0.063	0.049
4	41.065587	-101.099942	964.36	11.78	1899	0.090	0.027	31.12	-0.1814	0.338	0.225	0.068	0.157
5	41.066027	-101.098348	960.95	13.59	1899	0.090	0.027	36.07	-0.1623	0.342	0.152	0.069	0.083
6	41.065164	-101.103077	954.22	9.00	1899	0.090	0.027	33.49	-0.0894	0.296	0.104	0.055	0.049
7	41.066556	-101.101864	954.87	12.84	1899	0.090	0.027	37.28	-0.0858	0.302	0.111	0.049	0.062
8	41.066830	-101.104101	954.17	10.30	1899	0.090	0.027	36.22	-0.0727	0.245	0.080	0.073	0.007
9	41.067846	-101.102910	957.59	9.70	1899	0.090	0.027	38.11	-0.0599	0.304	0.050	0.043	0.007
10	41.068960	-101.103054	954.23	9.23	1899	0.090	0.027	36.75	-0.0823	0.285	0.078	0.051	0.027
11	41.068603	-101.104315	953.95	10.17	1899	0.090	0.027	39.07	-0.0579	0.211	0.083	0.065	0.018
12	41.067984	-101.105326	956.52	9.27	1899	0.090	0.027	37.89	0.0113	0.270	0.096	0.057	0.039
13	41.064118	-101.099389	964.24	10.82	1899	0.090	0.027	29.98	-0.0667	0.302	0.071	0.062	0.009
14	41.064344	-101.101150	960.25	10.61	1899	0.090	0.027	33.20	-0.0605	0.315	0.090	0.063	0.027
15	41.062904	-101.100508	961.18	8.56	1899	0.090	0.027	31.68	-0.1141	0.264	0.076	0.042	0.034
16	41.068032	-101.106028	955.85	12.16	1899	0.090	0.027	36.13	0.0007	0.326	0.142	0.048	0.094
17	41.067044	-101.106099	954.74	11.33	1899	0.090	0.027	43.32	0.0208	0.262	0.109	0.058	0.051
18	41.067116	-101.106920	955.13	10.41	2601	0.193	0.100	43.84	0.2084	0.347	0.217	0.062	0.155
19	41.065569	-101.106111	952.97	9.06	2601	0.193	0.100	47.80	0.1812	0.311	0.206	0.090	0.116
20	41.064355	-101.104755	953.11	8.69	2601	0.193	0.100	36.45	0.1285	0.348	0.175	0.056	0.119
21	41.065819	-101.104869	953.08	15.14	2601	0.193	0.100	43.80	0.0456	0.322	0.203	0.052	0.151
22	41.063784	-101.103113	954.26	10.35	9005	0.206	0.112	37.11	0.0877	0.337	0.222	0.084	0.138
23	41.062190	-101.103018	949.28	12.75	9002	0.206	0.112	47.89	0.1577	0.341	0.149	0.053	0.096
24	41.062758	-101.102466	952.23	11.45	9005	0.206	0.112	38.00	0.0651	0.321	0.113	0.044	0.069
25	41.062345	-101.103958	948.56	11.33	8867	0.225	0.125	45.50	0.2822	0.350	0.230	0.070	0.160
26	41.062963	-101.104660	948.52	11.81	8867	0.225	0.125	64.64	0.2607	0.345	0.223	0.054	0.169
27	41.062488	-101.105314	948.14	13.02	8867	0.225	0.125	56.64	0.2843	0.370	0.315	0.078	0.237
28	41.063059	-101.106123	949.00	12.00	2676	0.307	0.164	49.04	0.3139	0.347	0.241	0.087	0.154
29	41.063915	-101.106087	951.10	8.67	2594	0.168	0.068	42.25	0.2304	0.353	0.255	0.091	0.164
30	41.064106	-101.106992	951.25	11.34	2594	0.168	0.068	45.06	0.2350	0.368	0.302	0.114	0.188
31	41.065790	-101.107226	954.50	4.01	2601	0.193	0.100	42.86	0.2284	0.350	0.251	0.081	0.170

Table 2.1: Summary of undisturbed soil core locations and associated values.

2.3.3 Comparison of landscape position and hydrogeophysical datasets with laboratory analysis

Figure 2.8 illustrates scatterplots of AWC, elevation, TWI, ECa and EOF datasets with the measured field capacity and wilting point values measured from the soil water retention curves generated using the Hyprop and WP4C instruments. The first EOF coefficients have the largest linear correlation coefficient (r^2) with calculated AWC ($r^2 = 0.613$, Root mean squared error (RMSE) = $0.042 \text{ cm}^3\text{cm}^{-3}$), measured SWC at field capacity ($r^2 = 0.603$, RMSE = $0.048 \text{ cm}^3\text{cm}^{-3}$) and measured SWC at wilting point ($r^2 = 0.166$, RMSE = $0.015 \text{ cm}^3\text{cm}^{-3}$) (Table 2). Compared to ECa, the CRNP and EOF analysis increased the linear correlation r^2 by 0.218 and reduced the RMSE by $0.012 \text{ cm}^3\text{cm}^{-3}$ for measured SWC at field capacity. Table 2.2 also illustrates the weak relationship between measured SWC at field capacity and elevation ($r^2 = 0.297$, RMSE = $0.064 \text{ cm}^3\text{cm}^{-3}$), measured SWC at wilting point and elevation ($r^2 = 0.047$, RMSE = $0.016 \text{ cm}^3\text{cm}^{-3}$), calculated AWC and elevation ($r^2 = 0.321$, RMSE = $0.055 \text{ cm}^3\text{cm}^{-3}$), measured SWC at field capacity and TWI ($r^2 = 0.005$, RMSE = $0.076 \text{ cm}^3\text{cm}^{-3}$), measured SWC at wilting point and TWI ($r^2 = 0.011$, RMSE = $0.017 \text{ cm}^3\text{cm}^{-3}$), and calculated AWC and TWI ($r^2 = 0.012$, RMSE = $0.067 \text{ cm}^3\text{cm}^{-3}$). Therefore, the hypothesis that the first EOF provides superior spatial information correlating to the accurate prediction of three key soil hydraulic parameters is justified for this field.

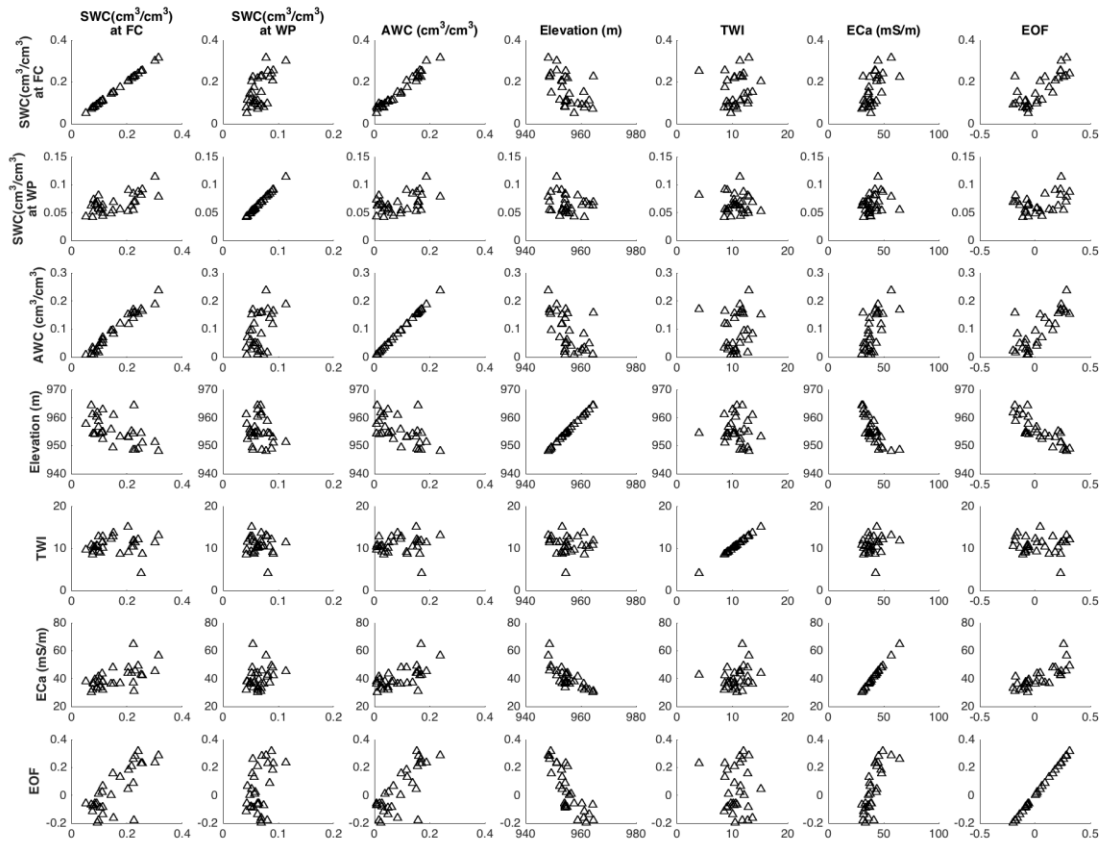


Figure 2.8: Laboratory measured SWC at field capacity (FC) and wilting point (WP) compared to AWC, elevation, TWI, measured ECa, and the first EOF surface from the CRNP rover SWC surveys.

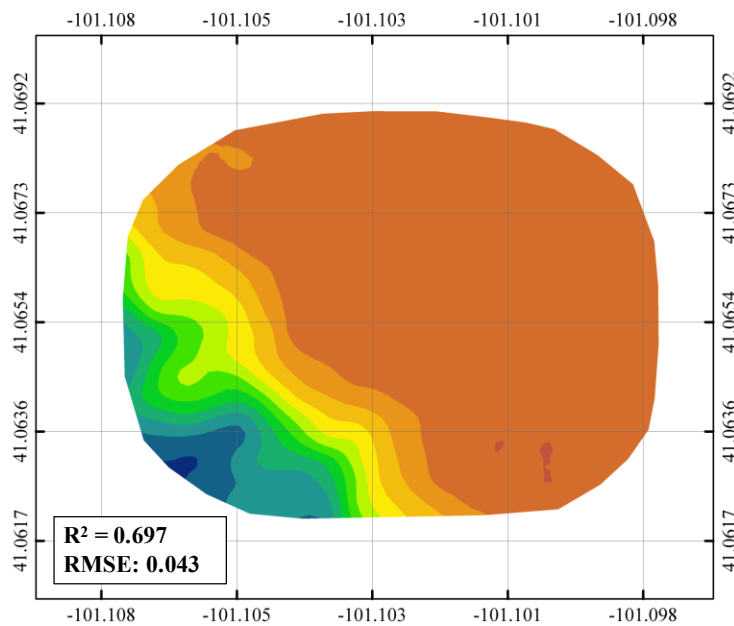
	Elevation (m)	TWI	ECa (mS/m)	EOF
SWC at Field Capacity (cm³/cm³)	r ² = 0.297, RMSE = 0.064	r ² = 0.005, RMSE = 0.076	r ² = 0.385, RMSE = 0.060	r ² = 0.603, RMSE = 0.048
SWC at Wilting Point (cm³/cm³)	r ² = 0.047, RMSE = 0.016	r ² = 0.011, RMSE = 0.017	r ² = 0.070, RMSE = 0.016	r ² = 0.166, RMSE = 0.015
AWC (cm³/cm³)	r ² = 0.321 RMSE = 0.055	r ² = 0.012 RMSE = 0.067	r ² = 0.411 RMSE = 0.051	r ² = 0.613 RMSE = 0.042

Table 2.2: Linear regression r^2 and RMSE for measured SWC at field capacity, measured SWC at wilting point and calculated AWC versus elevation, TWI, ECa map and EOF surface.

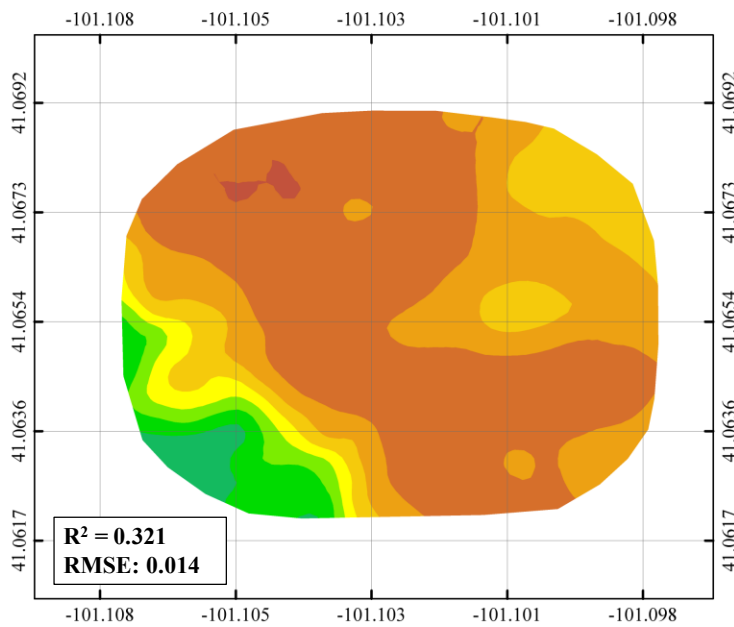
In addition to providing more accurate soil hydraulic property spatial datasets, EOFs can be used to generate new data products for use with VRI, VSI and other commercial field equipment. As an illustration here, new field capacity, wilting point and AWC products were generated for this field using the relationship between EOF and our observed hydraulic parameters (Figure 2.9). A second order polynomial was used to characterize the relationship between the measured SWC at field capacity ($r^2 = 0.697$, RMSE = 0.043 cm³cm⁻³), measured SWC at wilting point ($r^2 = 0.321$, RMSE = 0.014 cm³cm⁻³) and calculated AWC ($r^2 = 0.677$, RMSE = 0.039 cm³cm⁻³) with the first EOF surface. The authors note that additional single or multivariate linear/nonlinear functions could be explored to better characterize the observed trends in the data. These new data products could be used within current irrigation management practice to improve WUE by providing soil spatial datasets for the management of irrigation rates and times in relation to depletion below field capacity and above wilting point. Having an accurate

quantification of field capacity and wilting point is especially important when volumetric SWC sensors are used for irrigation management.

a) SWC ($\text{cm}^3\text{cm}^{-3}$)
at FC



b) SWC ($\text{cm}^3\text{cm}^{-3}$)
at WP



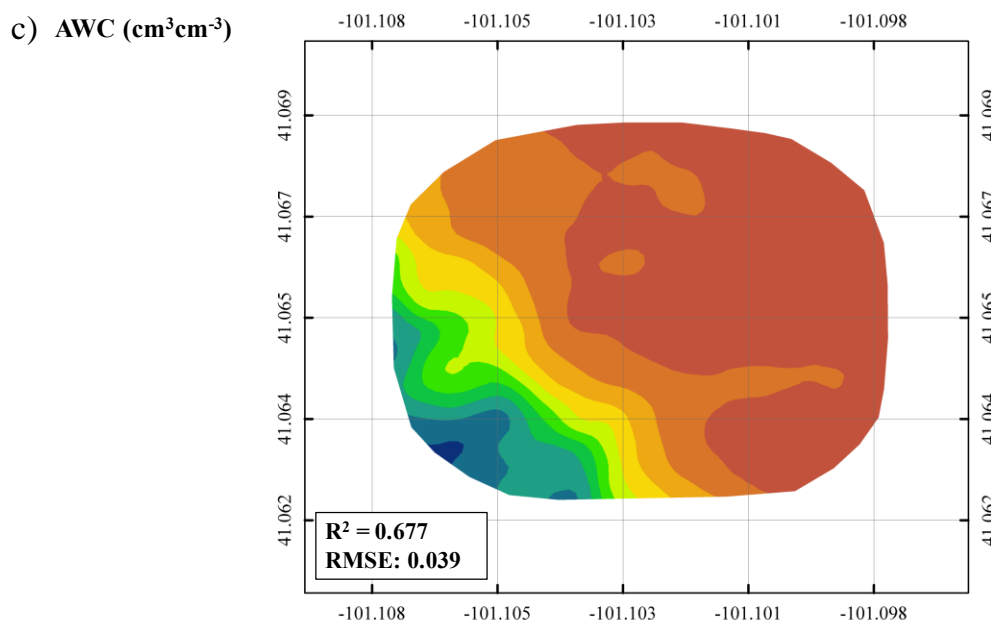


Figure 2.9: Resulting spatial estimates of a) SWC at field capacity, b) SWC at wilting point and c) AWC using derived relationship between laboratory measured soil hydraulic parameters and the first EOF surface.

2.3.4 Recommendations for future soil hydraulic property sampling

Given the results of this work the authors propose a sampling strategy for better quantifying soil hydraulic properties that can be implemented in practice. 1) Complete a minimum of 5 CRNP rover surveys for the area of interest, with survey datasets selected to capture a range of SWC, to accurately estimate spatial SWC using the first one or two sets of EOF coefficients. As previously stated, the presented work found five CRNP surveys at different SWC conditions were sufficient to estimate the first EOF coefficients to within 5% of the values using data from all ten surveys. A service provider could invest in CRNP technology and cooperate with multiple producers to perform the rover surveys. Additionally, the surveys could be completed simultaneously with other field operations (i.e. ATV, tractor, sprayer) and over several growing seasons. 2) Using the

EOF coefficients from the CRNP SWC maps, 7 – 8 soil sample locations should be selected across a range of EOF values. The collection and analysis of soil cores to determine their soil retention curves and hydraulic parameters can be time consuming, laborious and expensive. Therefore, using the EOF surface to minimize the number of and placement of extracted soil cores is critical. Here the authors suggest 7 – 8 soil sample cores based on the results that indicate a 2nd order polynomial relationship described the relationship best between the first EOF surface and measured SWC at field capacity ($r^2 = 0.697$, $RMSE = 0.043 \text{ cm}^3\text{cm}^{-3}$) and wilting point ($r^2 = 0.321$, $RMSE = 0.014 \text{ cm}^3\text{cm}^{-3}$). Based on additional data (Franz unpublished) from fields across the Midwest, the authors expect similar relationships and recommendations for the required minimal number of samples. 3) Next, measure the soil hydraulic properties of interest (i.e. field capacity, wilting point, AWC) for the collected soil samples. Soil samples can be sent to a soil laboratory or generated in one's lab using the Hyprop/WP4C combination for this work. 4) New data products can be generated using the relationship between EOF and the observed hydraulic parameters from the soil cores. These new data products can be generated at a variety of scales and file types to operate within existing agricultural software and machinery. 5) In addition, the EOF surface can be used to delineate management zones. This should be done in conjunction with the USDA SSURGO data to better refine key boundaries. IMZs can be based on the EOF surface, the field capacity surface or the AWC surface.

This research is of increasing importance for agricultural regions with ever-increasing water restrictions where small changes in water allocation rates and times may greatly impact crop yields. For example, at the current depletion rate, 35% of the

Southern High Plains Aquifer is expected to be unable to support irrigation in the next 30 years (Scanlon et al. 2012). Consequently, there will be an increased effort to accurately map soil hydraulic properties and delineate high spatial and temporal irrigation prescription maps. Referring to Figure 2.1, the feasibility of the CRNP and EOF analyses for management practice may soon be economically viable for many regions where maximizing water use for obtaining higher yields is paramount. The authors have shown the strong correlation with observed soil hydraulic parameters to the first EOF surface provides additional spatial variability information compared to EC mapping alone. If a land manager only used an EC map for estimating soil hydraulic properties, areas of a field may be biased depending on conditions at the time of sampling. In order to minimize error and improve IMZs, CRNP and EOF analysis should be used to increase the correlation between soil hydraulic properties and irrigation application rates (Figure 2.8, Table 2.2), which will subsequently improve irrigation prescription maps. CRNP and EOF analysis also provides irrigators with datasets they can use to generate dynamic prescription irrigation maps. Future research could investigate how increases in r^2 and reductions in RMSE using the CRNP and EOF analysis could translate into reduced pumping with precision agricultural technologies. Additionally, studies could investigate whether high spatial resolution datasets of soil hydraulic properties increase WUE while maintaining or increasing crop yields.

2.4 Summary and Conclusion

Irrigation constitutes the largest component in global water use, yet within agricultural systems there is low WUE. Therefore, improvements can be made in how

irrigation application rates and times are managed. Traditional methods include the use of available soil property datasets, EC mapping or commercially available instruments to delineate irrigation and land management zones. This research explored the utility of a relatively new hydrogeophysical sensor, called the CRNP, which measures near-surface SWC (top ~30 cm). In addition, when combining the CRNP SWC maps with the multivariate EOF analysis the authors found a better covariate for laboratory measured soil hydraulic properties for a field in west-central Nebraska, USA. The measured soil hydraulic properties were also compared to other readily available landscape and geophysical datasets including elevation, TWI and ECa maps. Based on these findings a future sampling strategy was proposed to better understand spatially varying hydraulic properties within a field, as well as delineation of IMZs. The authors do note that the strategy presented here constitutes a significant increase in effort as compared to more traditional and widely used techniques. However, as irrigation allocations become more stringent, there will likely be an increased rate of adoption of precision techniques that require more accurate mapping of soil hydraulic properties. The technology and framework presented here provides one potential strategy to better utilize precision agricultural technologies to increase WUE while maintaining crop yields in varying topographic landscapes.

Chapter 3: Conclusions & Future Directions

The major limitation to increasing agronomic outputs to meet future food and fiber demands is water scarcity. Consequently, global water security is dependent upon irrigation management. Precision agricultural technologies allow for land managers to vary irrigation rates and times within a field depending on soil physical properties. USDA soil datasets and EC mapping are traditional methods used for defining management zones. However, these datasets are not always an accurate representation of a field's soil spatial properties. The results presented in this thesis support the implementation of CRNP EOF analysis into agricultural practice because it more accurately delineates soil spatial structure for the writing of IMZs and irrigation prescription maps. Thus, CRNP EOF analysis has the potential to improve WUE.

Based on the results in Chapter 2, the following sampling strategy was recommended for better quantifying soil hydraulic properties that can be implemented in practice. 1) Complete a minimum of 5 CRNP rover surveys for the area of interest, with survey datasets selected to capture a range of SWC, to accurately estimate spatial SWC using the first one or two sets of EOF coefficients. The USDA offers guidelines one could follow to estimate a range of SWC based on a soil's feel and appearance. Alternatively, the dates for CRNP surveys could also be determined based on in-situ SWC sensors. 2) Using the EOF coefficients from the CRNP SWC maps, 7 – 8 soil sample locations should be selected across a range of EOF values. The locations could be chosen at equal intervals across the range of EOF values or in areas of the field with high spatial variability. 3) Next, measure the soil hydraulic properties of interest (i.e. field capacity, wilting point, AWC) for the collected soil samples. Soil samples can be sent to

a soil laboratory or generated in one's lab using the Hyprop/WP4C combination for this work. 4) New data products can be generated using the relationship between EOF and the observed hydraulic parameters from the soil cores. These new data products can be generated at a variety of scales and file types to operate within existing agricultural software and machinery. 5) The EOF surface can be used to delineate management zones. This should be done in conjunction with the USDA SSURGO data to better refine key boundaries. IMZs can be based on the EOF surface, the field capacity surface or the AWC surface.

Next, I will address a few limitations and potential solutions to the adoption of the CRNP EOF analysis into current irrigation management practice. 1) The upfront cost of a CRNP rover. As stated previously in Chapter 2, a service provider could invest in CRNP technology and cooperate with multiple producers to perform the rover surveys. By providing CRNP surveys as part of their services, the upfront cost of the CRNP sensor could be offset by prospective profits. The surveys could also be completed simultaneously with other field operations because the instrument can be mounted on most equipment used in field management. Additionally, multiple growing seasons could be used to complete the CRNP surveys for the EOF analysis. 2) Performing the CRNP EOF analysis. To address this, a simple MatLab code can be written. The program would allow the user to select the CRNP rover surveys they wished to include in the EOF analysis. The user would then run the code and the output file would be an EOF surface saved as a text or shapefile. 3) The effort required to implement the proposed sampling strategy above. A land manager may be okay with decreased accuracy in soil spatial variance determined by EOF values if the number of CRNP surveys needed could be

reduced. Future research could investigate the correlation between the number of CRNP surveys and variance in EOF values or delineated IMZs across multiple study sites. 4) Availability of commercial laboratories for analyzing the collected soil cores for soil hydraulic properties. Not every soils laboratory offers services for measuring soil hydraulic traits. Therefore, texture of the soil samples could be determined at a soils laboratory. Then, pedotransfer functions (PTF) could be used to approximate for desired parameters along the soil water characteristics curve. This approach may be a more cost-effective solution for some land managers.

Future directions for this work include the generation of VRI prescription irrigation maps for use in practice. Studies could investigate whether high spatial resolution datasets of soil hydraulic properties do increase WUE while maintaining or increasing crop yields. Irrigators can compare historical datasets with irrigation rates and crop yield using CRNP EOF IMZs. The additional effort required to implement this method may be deemed necessary as water resources undergo increasing regulation in the future. Implementing this method into current agricultural practice is the next step for increasing WUE in irrigated systems.

References

- Binley, A., Hubbard, S. S., Hulsman, J. A., Revil, A., Robinson, D. A., Singha, K., et al. (2015). The emergence of hydrogeophysics for improved understanding of subsurface processes over multiple scales. *Water Resources Research*, 51(6), 3837-3866. doi:10.1002/2015wr017016
- Bobryk, C. W., Myers, D. B., Kitchen, N. R., Shanahan, J. F., Sudduth, K. A., Drummond, S. T., et al. (2016). Validating a digital soil map with corn yield data for precision agriculture decision support. *Agronomy Journal*, 108(3), 957-965. doi:10.2134/agronj2015.0381
- Bogena, H. R., Huisman, J. A., Baatz, R., Franssen, H. J. H., & Vereecken, H. (2013). Accuracy of the cosmic-ray soil water content probe in humid forest ecosystems: The worst case scenario, *Water Resources Research*, 49(9), 5778-5791. doi:10.1002/wrcr.20463.
- Brevik, E. C., Fenton, T. E., & Lazari, A. (2006). Soil electrical conductivity as a function of soil water content and implications for soil mapping. *Precision Agriculture*, 7(6), 393-404. doi:10.1007/s11119-006-9021-x
- Chan, S., Njoku, E. G. & Colliander A. (2014). Soil Moisture Active Passive (SMAP), Algorithm Theoretical Basis Document, Level 1C Radiometer Data Product, Revision A, 20 pp, Jet Propulsion Laboratory, California Institute of Technology, Pasadena, CA. <http://smap.jpl.nasa.gov/>. Last accessed 15 February 2017.
- Decagon Devices, Inc. (2015). WP4C dewpoint potentiometer operator's manual. Pullman, WA.
- Dualem Inc. (2013). DUALEM-21S user's manual. Milton: Dualem Inc.
- Evans, R. G., Hans, S., & Kroger, M. W. (1996). Precision center pivot irrigation for efficient use of water and nitrogen. *Precision Agriculture*, 75-84.
- Franz, T. E., King, E. G., Caylor, K. K., & Robinson D.A. (2011). Coupling vegetation organization patterns to soil resource heterogeneity in a central Kenyan dryland using geophysical imagery. *Water Resources Research*, 47. doi:W07531 10.1029/2010wr010127.
- Franz, T. E., Wahbi, A., Vreugdenhil, M., Weltin, G., Heng, L., Oismueller, et al. (2016). Using cosmic-ray neutron probes to monitor landscape scale soil water content in mixed land use agricultural systems, *Applied and Environmental Soil Science, In Press*. doi:10.1155/2016/4323742
- Franz, T.E., Wang, T., Avery, W., Finkenbiner, C., & Brocca, L. (2015). Combined analysis of soil moisture measurements from roving and fixed cosmic-ray neutron probes for multiscale real-time monitoring. *Geophysical Research Letters*, 42(9), 3389-3396. doi:10.1002/2015gl063963

- Franz, T. E., Zreda, M., Rosolem, R. & Ferre, P. A. (2012). Field validation of cosmic-ray soil moisture sensor using a distributed sensor network, *Vadose Zone Journal*, 11(4). doi:10.2136/vzj2012.0046.
- Haghverdi, A., Leib, B. G., Washington-Allen, R. A., Ayers, P. D., & Buschermohle, M. J. (2015a). High-resolution prediction of soil available water content within the crop root zone. *Journal of Hydrology*, 520, 167-179. doi:10.1016/j.jhydrol.2015.09.061
- Haghverdi, A., Leib, B. G., Washington-Allen, R. A., Ayers, P. D., & Buschermohle, M. J. (2015b). Perspectives on delineating management zones for variable rate irrigation. *Computers and Electronics in Agriculture*, 117, 154-167. doi:10.1016/j.compag.2015.06.019
- Hawdon, A., D. McJannet, and J. Wallace (2014), Calibration and correction procedures for cosmic-ray neutron soil moisture probes located across Australia, *Water Resources Research*, 50(6), 5029-5043. doi:10.1002/2013wr015138.
- Hedley, C. (2015). The role of precision agriculture for improved nutrient management on farms. *Journal of the Science of Food and Agriculture*, 95(1), 12-19. doi:10.1002/jsfa.6734
- Hedley, C. B., Roudier, P., Yule, I. J., Ekanayake, J., & Bradbury, S. (2013). Soil water status and water table depth modelling using electromagnetic surveys for precision irrigation scheduling. *Geoderma*, 199, 22-29. doi:10.1016/j.geoderma.2012.07.018
- Hezarjaribi, A., & Sourell, H. (2007). Feasibility study of monitoring the total available water content using non-invasive electromagnetic induction-based and electrode-based soil electrical conductivity measurements. *Irrigation and Drainage*, 56(1), 53-65. doi:10.1002/ird.289
- Howell, T. A., Evett, S. R., O'Shaughnessy, S. A., Colaizzi, P. D., & Gowda, P. H. (2012). Advanced irrigation engineering: Precision and precise. *Journal of Agricultural Science and Technology*, A2, 1-9.
- Köhli, M., Schrön, M., Zreda, M., Schmidt, U., Dietrich, P., & Zacharias, S. (2015). Footprint characteristics revised for field-scale soil moisture monitoring with cosmic-ray neutrons. *Water Resources Research*, 51(7), 5772-5790. doi:10.1002/2015wr017169
- Korres, W., Koyama, C. N., Fiener, P., & Schneider, K. (2010). Analysis of surface soil moisture patterns in agricultural landscapes using empirical orthogonal functions. *Hydrology and Earth System Sciences*, 14(5), 751-764. doi:10.5194/hess-14-751-2010

- McCarthy, A. C., Hancock, N. H., & Raine, S. R. (2014). Development and simulation of sensor-based irrigation control strategies for cotton using the VARIwise simulation framework. *Computers and Electronics in Agriculture*, 101, 148-162. doi:10.1016/j.compag.2013.12.014
- McCutcheon, M. C., Farahani, H. J., Stednick, J. D., Buchleiter, G. W., & Green, T. R. (2006). Effect of soil water on apparent soil electrical conductivity and texture relationships in a dryland field. *Biosystems Engineering*, 94(1), 19-32. doi:10.1016/j.biosystemseng.2006.01.002
- McJannet, D., Franz, T., Hawdon, A., Boadle, D., Baker, B., Almeida, A., et al. (2014). Field testing of the universal calibration function for determination of soil moisture with cosmic-ray neutrons. *Water Resources Research*, 50(6), 5235-5248. doi:10.1002/2014wr015513
- Molden, D. (2007). Water responses to urbanization. *Paddy and Water Environment*, 5(4), 207-209. doi:10.1007/s10333-007-0084-8
- Pan, L., Adamchuk, V. I., Martin, D. L., Schroeder, M. A., & Ferguson, R. B. (2013). Analysis of soil water availability by integrating spatial and temporal sensor-based data. *Precision Agriculture*, 14(4), 414-433. doi:10.1007/s11119-013-9305-x
- Perry, M. A., & Niemann, J. D. (2006). Analysis and estimation of soil moisture at the catchment scale using EOFs. *Journal of Hydrology*, 334(3-4), 388-404. doi:10.1016/j.jhydrol.2006.10.014
- Peters, A., & Durner, W. (2008). Simplified evaporation method for determining soil hydraulic properties. *Journal of Hydrology*, 356(1-2), 147-162. doi:10.1016/j.jhydrol.2008.04.016
- Ranney, K. J., Niemann, J. D., Lehman, B. M., Green, T. R., & Jones, A. S. (2015). A method to downscale soil moisture to fine resolutions using topographic, vegetation, and soil data. *Advances in Water Resources*, 76, 81-96. doi:10.1016/j.advwatres.2014.12.003
- Rodríguez-Pérez, J. R., Plant, R. E., Lambert, J.-J., & Smart, D. R. (2011). Using apparent soil electrical conductivity (E_{Ca}) to characterize vineyard soils of high clay content. *Precision Agriculture*, 12(6), 775-794. doi:10.1007/s11119-011-9220-y
- Scanlon, B. R., Faunt, C. C., Longuevergne, L., Reedy, R. C., Alley, W. M., McGuire, V. L., et al. (2012). Groundwater depletion and sustainability of irrigation in the US High Plains and Central Valley. *Proceedings of the National Academy of Sciences of the United States of America*, 109(24), 9320-9325. doi:10.1073/pnas.1200311109

- Schindler, U., Durner, W., von Unold, G., Mueller, L., & Wieland, R. (2010). The evaporation method: Extending the measurement range of soil hydraulic properties using the air-entry pressure of the ceramic cup. *Journal of Plant Nutrition and Soil Science*, 173(4), 565-572. doi:10.1002/jpln.200900201
- Sorensen, R., Zinko, U., & Selbert, J. (2006). On the calculation of the topographic wetness index: Evaluation of different methods based on field observations. *Hydrology and Earth System Sciences*, 10, 101-112.
- Schultz, B., Thatte, C. D., Labhsetwar, V. K. (2005). Irrigation and drainage: Main contributors to global food production. *Irrigation and Drainage*, 54, 263–278.
- Soil Survey Staff (2016). Natural Resources Conservation Service, United States Department of Agriculture. Soil Survey Geographic (SSURGO) Database. <https://sdmdataaccess.sc.egov.usda.gov>. Accessed 1 February 2016.
- UNDP (2007). Human Development Report 2006- Beyond scarcity: power, poverty and the global water crisis. United Nations Development Programme, New York.
- USDA NASS (2007). Census of Agriculture. United States Department of Agriculture. https://www.agcensus.usda.gov/Publications/2007/Full_Report/usv1.pdf. Accessed 26 January 2017.
- Werbylo, K. L., & Niemann, J. D. (2014). Evaluation of sampling techniques to characterize topographically-dependent variability for soil moisture downscaling. *Journal of Hydrology*, 516, 304-316. doi:10.1016/j.jhydrol.2014.01.030
- Zreda, M., Shuttleworth, W. J., Zeng, X., Zweck, C., Desilets, D., Franz, T., et al. (2012). COSMOS: the COsmic-ray Soil Moisture Observing System. *Hydrology and Earth System Sciences*, 16(11), 4079-4099. doi:10.5194/hess-16-4079-2012

Appendix

Please note, all digital files can be requested from me (c.finkenbiner@gmail.com) or Dr. Franz (tf Franz2@unl.edu). Below are soil water retention functions for each of the undisturbed soil samples and the MatLab code that can be adapted to create these figures.

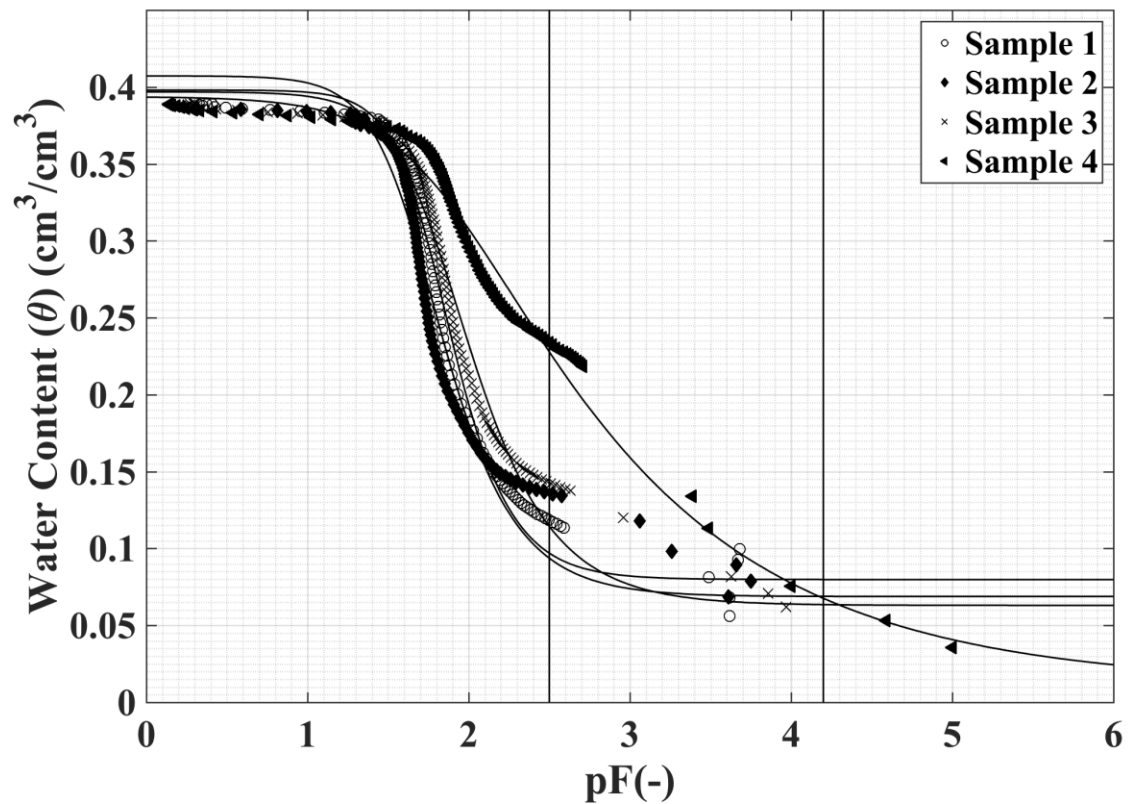


Figure S2.1: Soil water retention functions for undisturbed soil core samples 1, 2, 3 and 4. Values before pF (log of tension, (MPa)) of 2.8 were recorded using the Decagon Hyprop and values after a pF of 2.8 were recorded using a WP4C Dewpoint PotentialMeter.

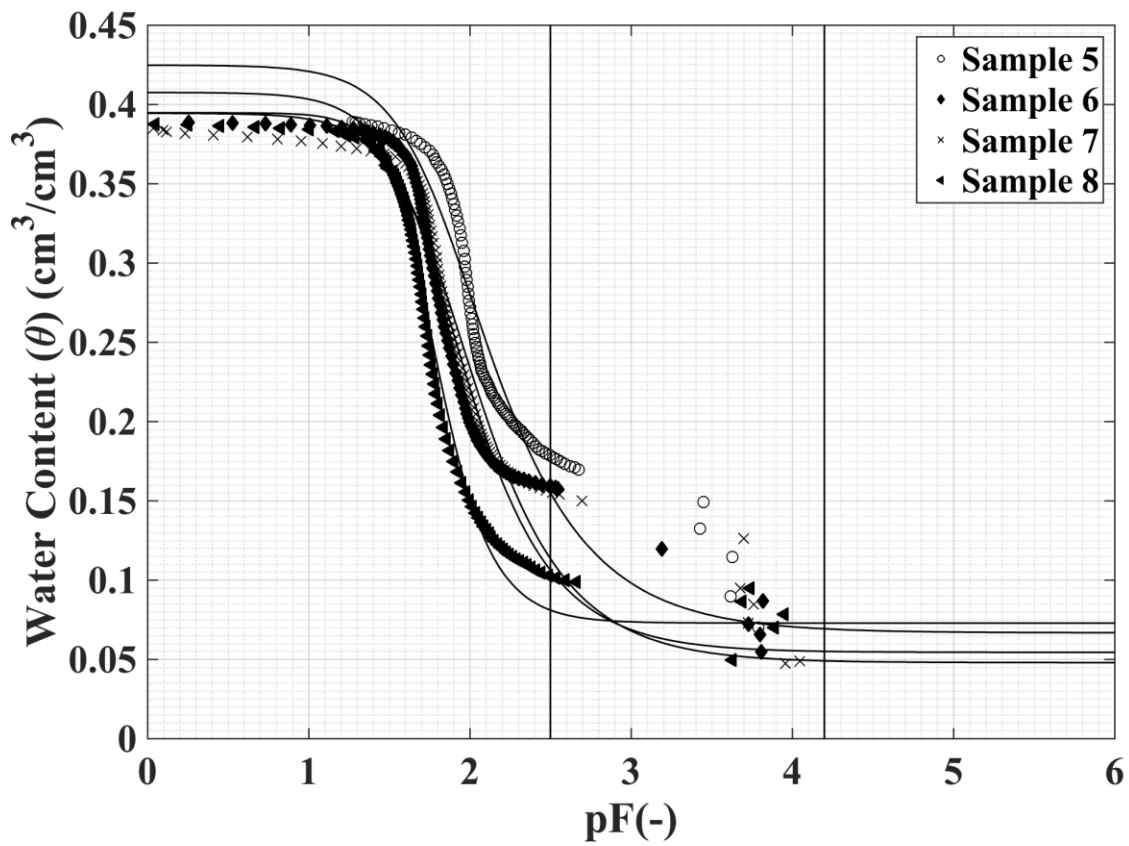


Figure S2.2: Soil water retention functions for undisturbed soil core samples 5, 6, 7 and 8. Values before pF (log of tension, (MPa)) of 3 were recorded using the Decagon Hyprop and values after a pF of 3 were recorded using a WP4C Dewpoint PotentialMeter.

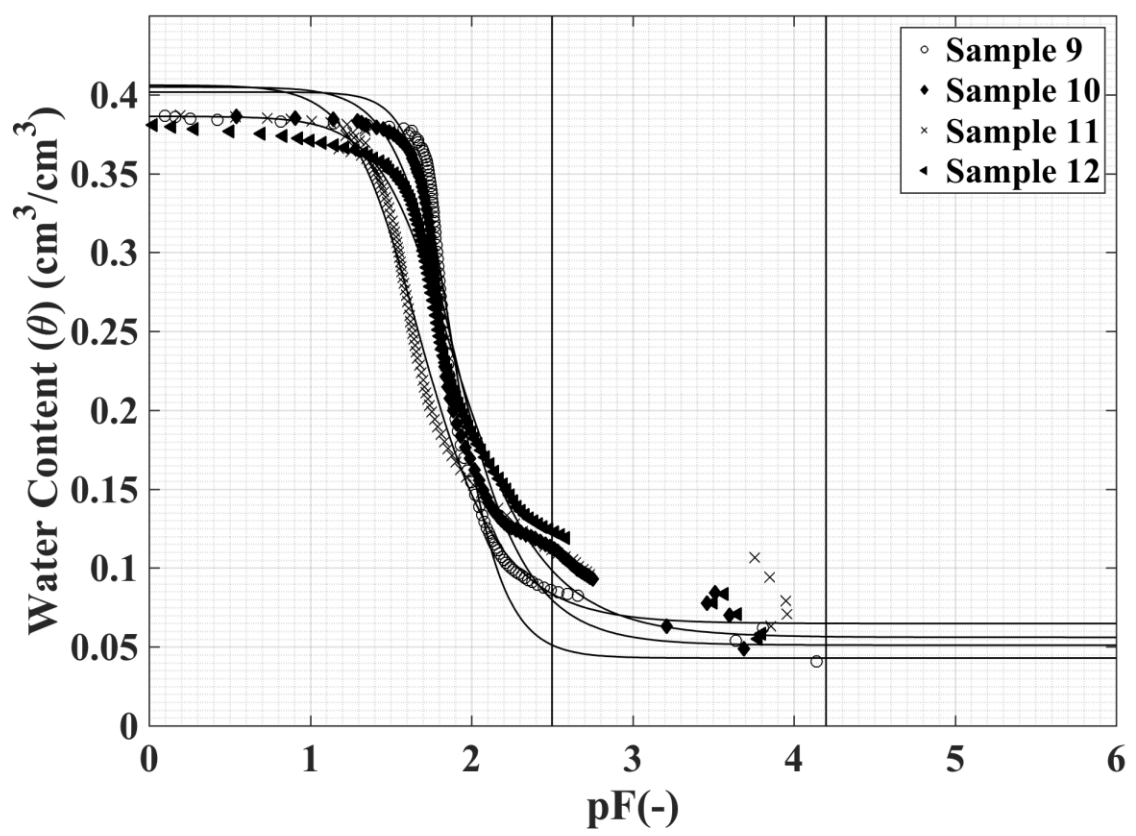


Figure S2.3: Soil water retention functions for undisturbed soil core samples 9, 10, 11 and 12. Values before pF (log of tension, (MPa)) of 3 were recorded using the Decagon Hyprop and values after a pF of 3 were recorded using a WP4C Dewpoint PotentiaMeter.

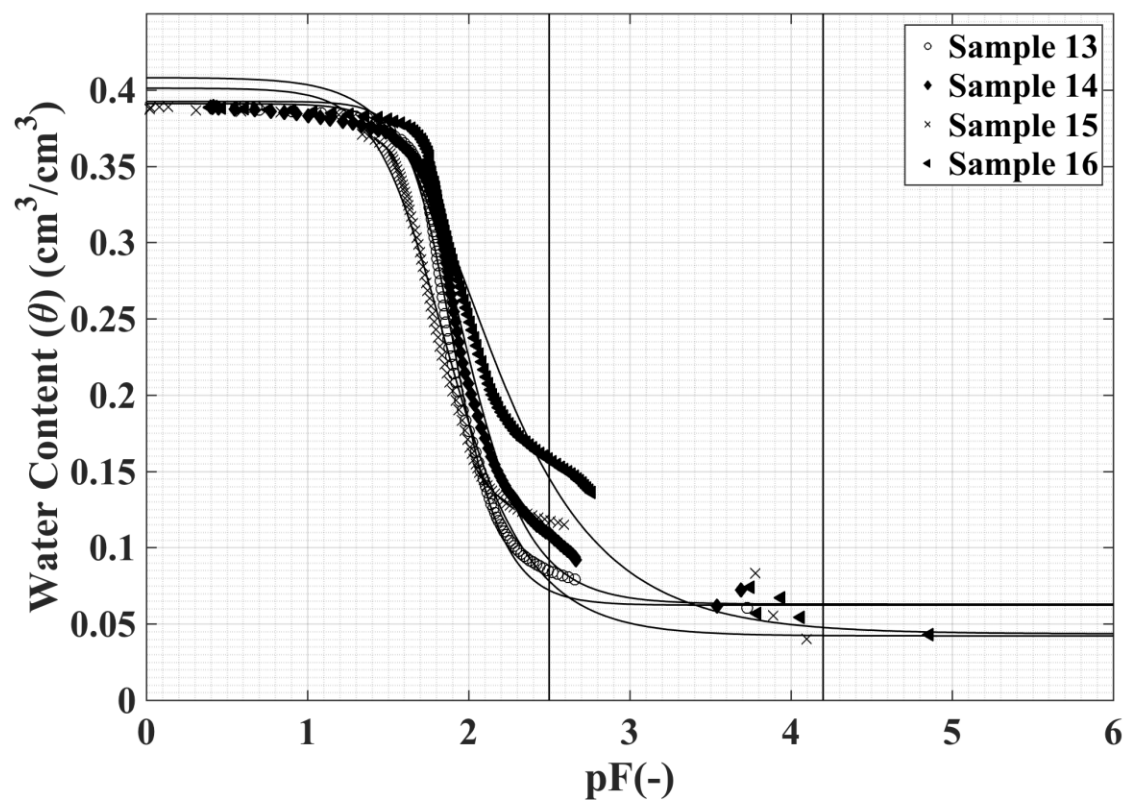


Figure S2.4: Soil water retention functions for undisturbed soil core samples 13, 14, 15 and 16. Values before pF (log of tension, (MPa)) of 3 were recorded using the Decagon Hyprop and values after a pF of 3 were recorded using a WP4C Dewpoint PotentialMeter.

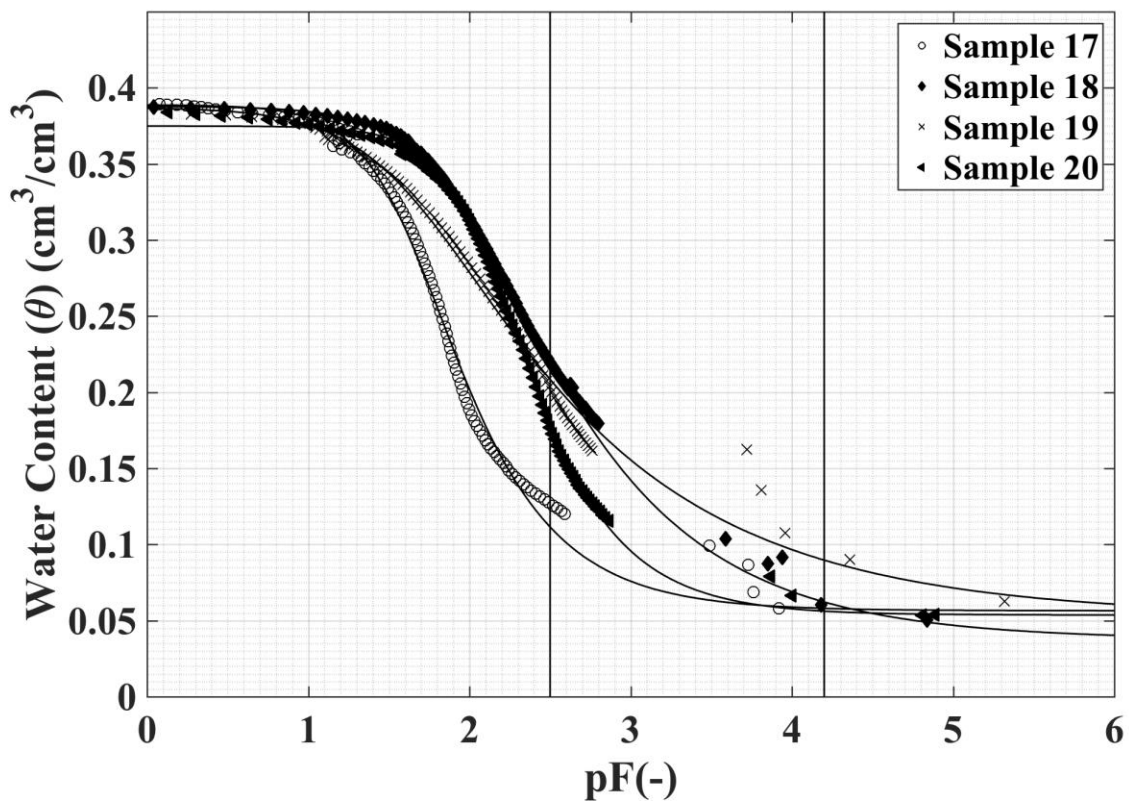


Figure S2.5: Soil water retention functions for undisturbed soil core samples 17, 18, 19 and 20. Values before pF (log of tension, (MPa)) of 3 were recorded using the Decagon Hyprop and values after a pF of 3 were recorded using a WP4C Dewpoint PotentiaMeter.

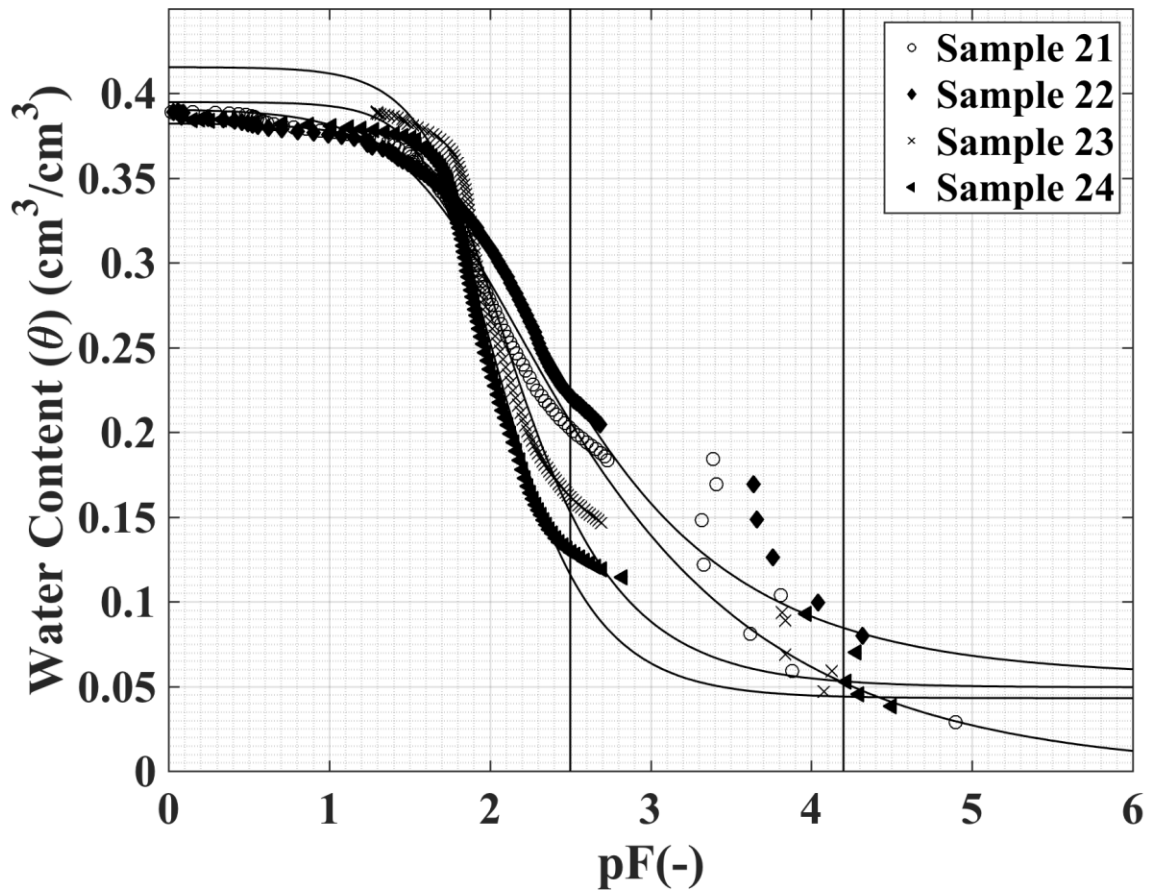


Figure S2.6: Soil water retention functions for undisturbed soil core samples 21, 22, 23 and 24. Values before pF (log of tension, (MPa)) of 3 were recorded using the Decagon Hyprop and values after a pF of 3 were recorded using a WP4C Dewpoint PotentialMeter.

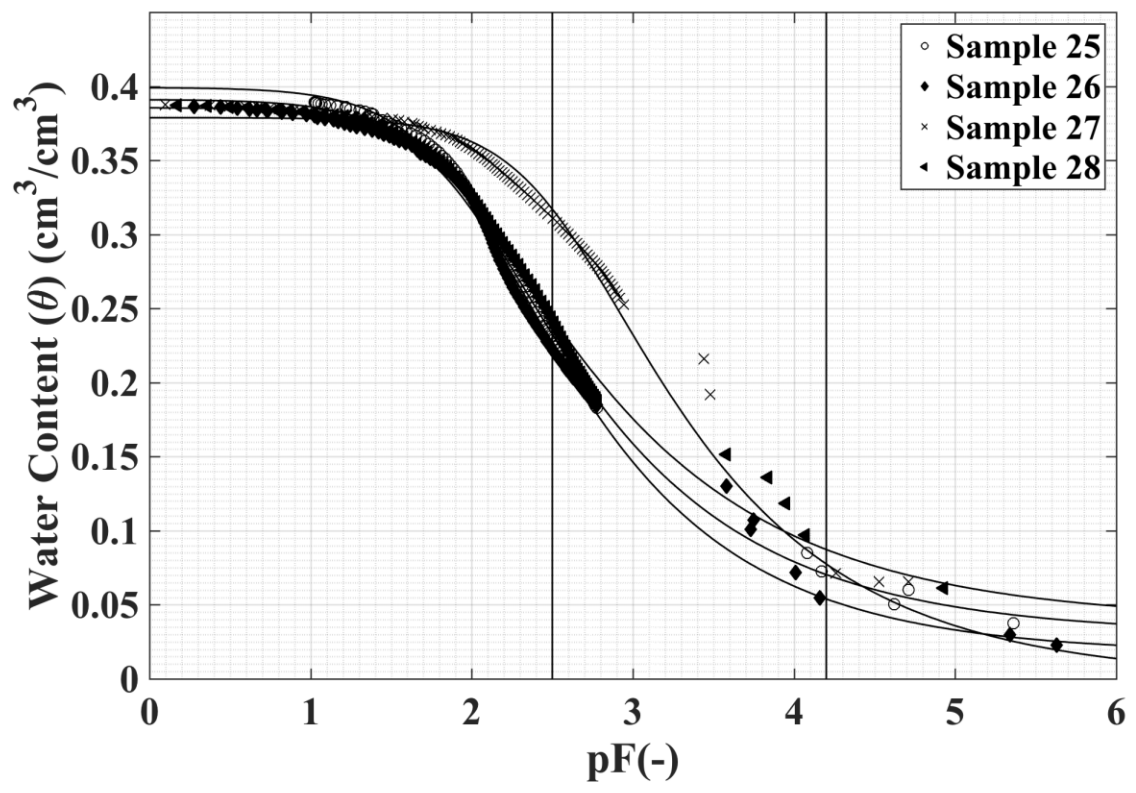


Figure S2.7: Soil water retention functions for undisturbed soil core samples 25, 26, 27 and 28. Values before pF (log of tension, (MPa)) of 3 were recorded using the Decagon Hyprop and values after a pF of 3 were recorded using a WP4C Dewpoint PotentialMeter.

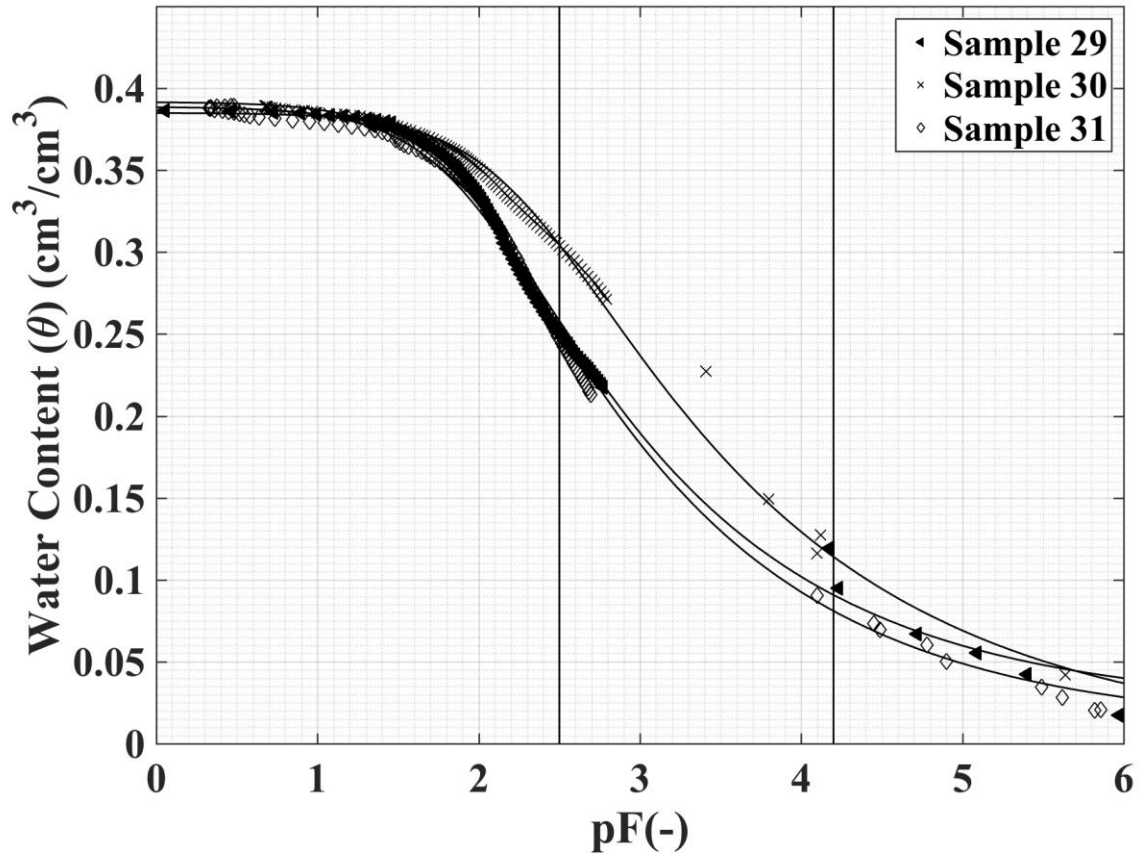


Figure S2.8: Soil water retention functions for undisturbed soil core samples 29, 20, and 31. Values before pF (log of tension, (MPa)) of 3 were recorded using the Decagon Hyprop and values after a pF of 3 were recorded using a WP4C Dewpoint PotentialMeter.

```

% Code will read text files of Hyprop & WP4C Curves
% Last Updated 03/13/2017

clc;
close all;
clear all;

% This program is intended for MS Thesis.
% Documents/Precicion_Ag_Manuscript/Hyprop Data/DataTextFiles

% Headers for the text files are labeled so: S1pF1, S1WC1, S1pF2, S1WC2
% S1pF1 = pF for Hyprop & WP4C data for sample 1 % S1 = sample 1
% S1WC1 = water content (cm3/cm3) for Hyprop & WP4C data for sample 1
% S2pF2 = pF for Hyprop & WP4C fitted curve for sample 1
% S2WC2 = water content (cm3/cm3) for Hyprop & WP4C fitted curve for sample 1

% T = tdfread('S1_retentioncurves.txt','');

F = dir('*.txt');
for ii = 1:length(F)
    fid = fopen(F(ii).name);
    tdfread(F(ii).name);
end

% Code to create figures from imported data above
% To change graphed samples, just change variable numbers with corresponding sample
% number

figure;
hold on;
set(gcf,'color','w');
axis([0,7,0,0.45]);

% Sample 2 Valent Sand 1899
f1 = scatter(S2pF1,S2WC1,'o','k','sizedata',85);
f2 = plot(S2pF2,S2WC2,'k','linewidth',1.5);
% Sample 16 Sandy Loam 8867
f3 = scatter(S16pF1,S16WC1,'d','r','sizedata',85);
f4 = plot(S16pF2,S16WC2,'r','linewidth',1.5);
% Sample 28 Silt Loam 2676
f5 = scatter(S28pF1,S28WC1,'x','b','sizedata',85);
f6 = plot(S28pF2,S28WC2,'b','linewidth',1.5);
legend([f1 f3 f5],'Sample 2','Sample 16','Sample 28');

%title('Soil Water Characteristics Curves');
set(gca,'fontsize',20,'fontweight','bold','fontname','Times New Roman');
set(gca,'linewidth',1.2)
yL = get(gca,'YLim');
line([2.5 2.5],yL,'Color','k','linewidth',1.5);
line([4.2 4.2],yL,'Color','k','linewidth',1.5);
xlabel('pF(-)');
ylabel('Water Content (\theta) (cm^3/cm^3)');
box on;
grid on;
grid minor;

```

Figure S2.9: MatLab (.m) script used to generated soil retention function figures for the undisturbed soil cores.